Interaction of low-energy antiprotons with nuclei

O. D. Dal'karov and V. A. Karmanov

P. N. Lebedev Physics Institute, USSR Academy of Sciences, Moscow

Fiz. Elem. Chastits At. Yadra **18**, 1399–1439 (November–December 1987)

The first results on the interaction of antiprotons with nuclei obtained in experiments at the Low Energy Antiproton Ring (LEAR) put into operation at CERN at the end of 1983 are presented and analyzed. In contrast to the case with protons of the same energy (~ 50 MeV), elastic $\bar{p}$–nucleus scattering manifests a pronounced diffractive nature and is described well by the Glauber–Sitenko approximation taking into account the Coulomb interaction. The effective nuclear radius determined from antiproton scattering is significantly (1.5 times for ^{12}C) larger than the radius determined from proton and electron scattering. We discuss the possible reasons for the applicability of the Glauber–Sitenko approach for antiprotons at such low energies. We show that it is possible to determine the parameters of the $\bar{p}N$ amplitude (in particular, the ratio of its real and imaginary parts) from the nuclear data. Data on the yield of ^{3}He nuclei in $\bar{p}^4$He annihilation are presented. The $\bar{p}$–nucleus optical potential is analyzed. We discuss the phenomenon of the cancellation between off-shell and nonadiabatic effects in the amplitude of the reaction $\bar{p}d \to e^+e^-n$, which leads to specific experimental consequences. The $\bar{p}$–nucleus scattering lengths and level shifts of antiprotonic atoms are discussed.

INTRODUCTION

In recent years the study of the antiproton interaction at low energies (from several MeV to ~ 100 MeV) with nuclei has entered a qualitatively new stage, signaled by the appearance of a new, independent field—low-energy antiproton physics. To a considerable degree, this field owes its existence to the fundamentally new experimental possibilities created by the operation, beginning in mid-1983, of a unique low-energy antiproton storage ring-LEAR (Low Energy Antiproton Ring) at CERN. In contrast to, for example, the $Sp\bar{p}S$ collider, in this storage ring antiprotons are not accelerated. On the contrary, they are decelerated to almost zero energy (the minimum antiproton momentum is 100 MeV/c, i.e., the minimum energy is ~ 5 MeV). The other difference is the successful extraction of an antiproton beam at LEAR, with the momentum of the antiprotons in the beam varying from 100 MeV/c to 1 GeV/c. The antiproton beam at LEAR has an important advantage over the currently existing antiproton beams at Brookhaven (USA) and KEK (Japan): it is nearly monoenergetic over the entire momentum range, and its intensity, especially at low momenta ($\lesssim 300$ MeV/c), is $6 \cdot 10^5$ $\bar{p}/c$, which on the average is 10 000 times greater than the intensity of the other beams. The resolution attained at present is already $\Delta p/p \sim 10^{-3}$; however, there are plans to introduce electron cooling in the next year or two (planned for the end of 1987), which will make it possible to obtain a resolution of order $\Delta p/p \sim 10^{-5}$–10^{-6}.

A set of statistics which formally took months or years to obtain can now be obtained at LEAR in a few hours. Of course, the creation of such a unique tool for study using low-energy antiprotons must give rise to qualitatively new theoretical ideas. This has been confirmed by the first experiments[1] on low-energy antiproton scattering on nuclei carried out at LEAR and the subsequent activity of theoreticians attempting to understand how nuclei "look" to antiprotons. As a result, it has become clear that antiproton–nucleus scattering can be very helpful for solving a number of problems in nuclear physics. Some of these are described below.

1. Study of the nuclear reaction mechanism

In the scattering of hadrons on nuclei there are several problems which seem to be tangled up into a single, unyielding knot. For example, the Glauber–Sitenko approach,[2,3] which has successfully been used for analyzing hadron–nucleus scattering at high energies ($\gtrsim 1$ GeV), is applicable when two basic conditions are satisfied simultaneously: a) the trajectory of the hadron in the nucleus should be a straight line (the eikonal approximation); b) it should be possible to neglect the motion of the intranuclear nucleons during the time of passage of the hadron through the nucleus (the adiabatic approximation). In particular, the rescattering of intranuclear nucleons on each other is neglected. Experience with calculations shows that both of these approximations work considerably better than might have been expected from simple estimates. It has been found[4] (Fig. 1) that in the case of antiprotons the Glauber–Sitenko mechanism[2,3] remains valid up to energies of ~ 50 MeV, whereas in the case of proton scattering at this energy it is in sharp conflict with experiment. Why does this happen, and what is the actual range of applicability of the Glauber–Sitenko approach?

In order to answer these questions, it is necessary to separately study the range of applicability of each of the approximations listed above. It is impossible to do this for a proton beam, because conditions (a) and (b) are satisfied or violated simultaneously, depending only on how large or small the incident hadron momentum is. Conditions (a) and (b) can be separated when antiprotons are used. The reason is that low-energy $\bar{p}N$ scattering is very strongly directed forward; moreover, the slope of the diffraction peak[1)] grows with decreasing energy. For comparison, the slope of the diffraction peak in $\bar{p}p$ scattering[5] is 35.6 (GeV/c)^2 at an energy of ~ 50 MeV, while elastic pp scattering at 50 MeV is practically isotropic.[6] The slope of the diffraction peak in pp scattering at energies above 1 GeV is no greater than 6 (GeV/c)^2, while the slope in $\bar{p}p$ scattering is no greater than 15 (GeV/c)^2 even at superhigh energies (at the collider energy, i.e., ~ 100 TeV in the laboratory frame). We note that

 0090-4759/87/060599-18$04.40

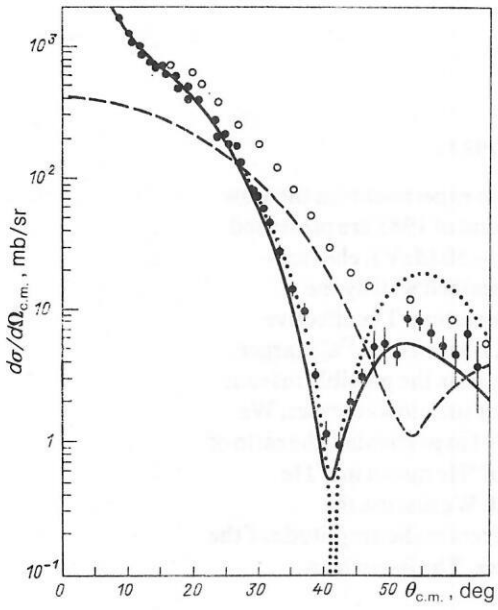

FIG. 1. Elastic differential cross sections for $\bar{p}^{12}$C (solid line) and p^{12}C (dashed line) scattering at kinetic energy $T_{\bar{p}} = 46.8$ MeV. The dotted line is the $\bar{p}^{12}$C cross section in the model of a perfectly black sphere [Eq. (16) for $R_{ef} = 3.96$ F]. The experimental data are from Ref. 1.

up to now such large values of the slope have been encountered only in the scattering of hadrons on nuclear targets (for example, in π^{-4}He scattering for the π^- meson energy roughly equal to 200 GeV; see the summary of the data in Ref. 7). This feature peculiar to $\bar{p}N$ scattering can ensure that condition (a) holds when there is no apparent reason for condition (b) to be satisfied, i.e., it offers a unique possibility of independently determining, on the basis of experimental data, the applicability of the adiabatic approximation. For the first time these two problems are separated.

It should be noted that many very curious facts have been discovered in the theoretical study of the mechanism for hadron scattering on nuclei. Many seemingly unrelated effects (for example, rescatterings of intranuclear nucleons and departure from the mass shell in amplitudes) almost completely cancel each other.[8] Any attempt to improve the Glauber–Sitenko approximation by including only one of these effects only makes the result worse. These facts, which were discovered in scattering on deuterons, up to now have been viewed as isolated and limited observations, and it has not been entirely clear whether or not they would survive when more complicated graphs were taken into account and in the case of heavier nuclei. Moreover, there are esthetic grounds for seeking the deep reasons for these phenomena: when one observes that several important contributions cancel, it is impossible to escape the feeling that there must exist some theory in which these contributions are absent from the start. It is with these troubling questions that we come to antiproton–nucleus scattering, but under conditions more favorable to an accurate experiment and with a new tool—the antiproton.

2. The study of nuclear structure

Since the mechanism for low-energy antiproton scattering on nuclei is given by the Glauber–Sitenko approach, that is, it is considerably simpler than in the case of protons, antiprotons offer new possibilities for studying nuclear structure. In addition, the following important fact has been discovered in $\bar{p}^{12}$C inelastic scattering with the excitation of levels of the residual nucleus[1]: in the spectrum of nuclear level excitation by antiprotons the continuum is significantly smaller than in the reaction ^{12}C$(p,p')^{12}$C*. In Fig. 2 we show the nuclear excitation spectrum in the reaction ^{12}C$(\bar{p},\bar{p}')^{12}$C* for fixed emission angle of the scattered antiproton. We clearly observe levels with energies 4.44, 9.64, and 15.1 MeV, two of which (9.64 and 15.1 MeV) lie in the continuum (owing to the absence of a rule which energetically forbids the breakup of the nucleus). We see that antiprotons cause the peaks corresponding to nuclear level excitation to be very sharp. There is less contrast when the nucleus is "seen" by a proton. For comparison, the differen-

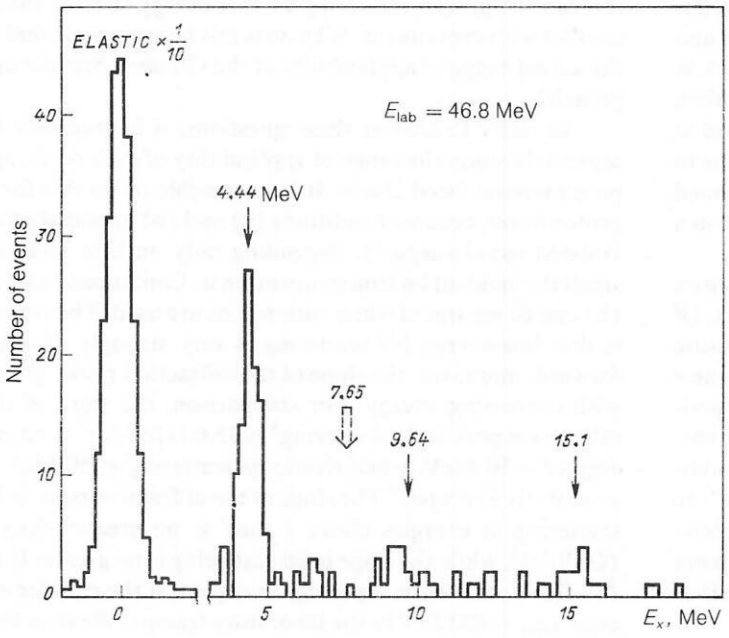

FIG. 2. Energy spectrum for the excitation of final states in $\bar{p}^{12}$C scattering at the angle 25° (Ref. 1). The number of events is plotted as a function of the excitation energy of the residual ^{12}C nucleus. The elastic peak is decreased by a factor of 10.

tial cross section in the continuum near 10 MeV for protons is 0.66 mb/(sr·MeV) at the angle 35° and 0.75 mb/(sr·MeV) at 25°, while for antiprotons these cross sections are no greater than 0.1 mb/(sr·MeV) (Ref. 1). This fact is very interesting for nuclear physics, since it indicates that it is possible in principle to study states lying in the continuum (such as giant resonances in heavy nuclei) under much more favorable background conditions.

3. Determination of the parameters of the $\bar{p}$–N amplitude from nuclear data

The most ill-determined parameter of the $\bar{p}N$ amplitude is the ratio ε of its real and imaginary parts. This ratio is usually found from very difficult experiments based on interference between the Coulomb and strong interactions. The data of different groups contradict each other (Fig. 3). Owing to multiple rescatterings of the antiproton on the intranuclear nucleons, in the nucleus the $\bar{p}N$ amplitudes corresponding to scattering on different nucleons interfere, even when the Coulomb interaction is absent. The cross section at the diffraction minima is proportional to ε^2 (Ref. 4). The inclusion of the Coulomb interaction between the antiproton and the nucleus, which is very important at low energies, distorts this dependence, but does not weaken it. Here the antiproton–nucleus interaction plays the role of an arbitrator and makes it possible to decide which value of ε is the true one. Getting ahead of ourselves, we note that the nuclear data display a preference for the value of ε obtained at LEAR.

To reliably extract the parameters of the $N\bar{N}$ amplitudes from the nuclear data we need to be confident of the mechanism for the process and to have reliable data on the properties of the nucleus (the density, transition form factors, and so on). Therefore, investigation in the three directions discussed above actually corresponds to the study of a single problem.

We now have a clear idea of the problems confronting us in this new field of investigation, that of antiproton interactions with nuclei. In the present study we shall discuss these problems and present the results which have been obtained.

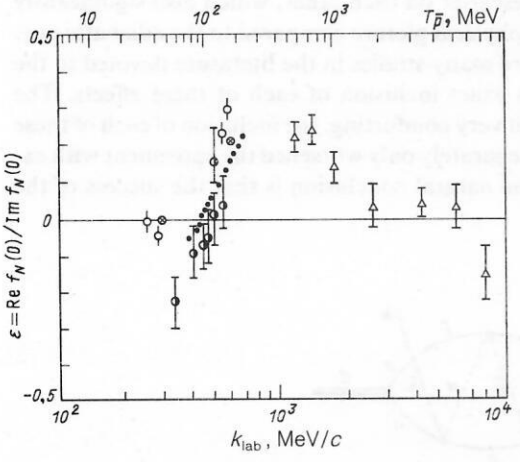

FIG. 3. The ratio ε of the real and imaginary parts of the $\bar{p}N$ amplitude: ○—LEAR data of Ref. 24; ◑—data of Ref. 29; ●—data of Ref. 61; △—data of Ref. 62; ⊗—values of ε obtained in Ref. 4 from $\bar{p}$–nucleus data.

In Sec. 1 we discuss in detail the conditions for the applicability of the Glauber–Sitenko approximation and the phenomenon of the cancellation of the various corrections to it. In Sec. 2 we review the Glauber–Sitenko formalism for elastic scattering and use it to analyze the data of Ref. 1 on antiproton scattering on the nuclei ^{12}C, ^{40}Ca, and ^{208}Pb and the KEK and BNL data for ^{27}Al and ^{64}Cu. In Sec. 3 we discuss the $\bar{p}$–nucleus optical potential. In Sec. 4 we analyze the reaction cross section $\sigma_r = \sigma_{tot} - \sigma_{el}$. In Sec. 5 we begin by giving the formulas for the amplitude of antiproton scattering on nuclei with the excitation of a level of the final nucleus. These formulas, in which all the information about the level excitation process is contained in the electromagnetic transition form factor, are obtained in the approximation of a single inelastic collision which amounts to the greatest possible simplification of the basic formulas of the Glauber–Sitenko theory. The calculations are then compared with the LEAR data on the antiproton excitation of the 2^+ level (4.44 MeV) of the nucleus ^{12}C. In Sec. 6 we study the annihilation reaction $\bar{p}d \to e^+e^-n$, whose amplitude also contains curious cancellations which lead to nontrivial experimental consequences. We also present the LEAR data on the yield of ^{3}He nuclei in $\bar{p}$ annihilation on ^{4}He. In Sec. 7 we discuss the antiproton scattering lengths for the nuclei ^{12}C and ^{16}O and compare the level shifts of antiprotonic atoms calculated using these data with experiment. In the concluding section we sum up the results and briefly discuss the problems confronting theory and experiment.

1. THE APPLICABILITY OF THE GLAUBER–SITENKO APPROXIMATION

In the Glauber–Sitenko theory[2,3] the picture of particle scattering on nuclei is in close analogy with optics: An incident particle, or rather, a plane wave similar to a flux of light rays, passes through a nucleus, scattering on the nucleons of the nucleus and being partially absorbed by them. The nucleons are assumed to be stationary during the time of passage of the particles of the nucleus, that is, it is as though the particle takes an instantaneous photograph of the nucleus. The scattering amplitude is obtained by averaging over all positions of the scatterers (nucleons). As discussed above, this picture assumes that the eikonal and adiabatic conditions are satisfied simultaneously.

a) The eikonal approximation. The conditions under which the eikonal approximation is valid and the corrections to it have been discussed in Refs. 9–16 and 71. For small momentum transfer $qR \lesssim 1$ the eikonal approximation is valid for $kR \gg 1$. In other words, the wavelength of the incident beam $\lambda = 1/k$ must be much smaller than the size of the nucleus. However, if $qR \gg 1$, the eikonal approximation is valid only when a stronger condition is satisfied[13]: $kR \gg (1/8)(qR)^2$. These conditions are satisfied in, for example, the scattering of protons of energy roughly equal to 1 GeV on nuclei. In this case the Glauber–Sitenko approximation gives a good description of the experimental data.[17] From Fig. 1 (open circles and dashed line) we see that at energies of around 50 MeV proton–nucleus scattering is not described by the Glauber–Sitenko theory and is not at all diffractive in nature. This seems natural, because at low energies none of the conditions listed above is, at first glance, satisfied. The energy 50 MeV corresponds to an incident-

nucleon momentum of the order of 300 MeV/c, which is comparable to the momenta of the intranuclear nucleons. On the other hand, as seen from Fig. 1, at this energy the scattering of antiprotons on ^{12}C is strongly diffractive in nature and is described well by the Glauber–Sitenko theory. One arrives at the same conclusion after analyzing antiproton scattering on the nuclei ^{40}Ca and ^{208}Pb at energies of 48.6 MeV and around 180 MeV (see below). It can be assumed that in this case the validity of the eikonal approximation is a consequence of the extremely narrow forward cone in $\bar{p}N$ scattering. More simply, it can be stated that a low-energy antiproton moves along a straight line, because it cannot be scattered off to the side.

We note that the appearance of such a narrow cone at low energies and its further narrowing with decreasing energy are themselves consequences of the fact that even at very low energies in $\bar{N}N$ scattering the contributions of several partial waves corresponding to nonzero orbital angular momenta are important. As was shown in Ref. 18, this phenomenon is not related to annihilation processes, but can be attributed to the presence of the spectrum of quasinuclear $\bar{N}N$ states corresponding to nonzero orbital angular momenta l of the relative motion of the N and $\bar{N}$ (levels are predicted in practically all spin–isospin states[19]). This is what leads to the significant enhancement of the contribution to low-energy $\bar{p}p$ scattering from partial waves up to $l = 3$. The total number of partial waves (taking into account the various spin–isospin states) is $\gtrsim 20$. Interference between partial waves causes low-energy $\bar{p}N$ scattering to be strongly directed forward.

The angular distributions in $\bar{p}N$ scattering have also been described in other models by means of the construction of an annihilation potential.[64–66]

We stress the fact that the amplitude of $\bar{p}N$ scattering behaves dramatically as a function of the momentum transfer. It is this dependence which enters into the Glauber–Sitenko formulas. This dependence is softened in the angular distributions, but still remains much more prominent than in pp scattering at the same energies.[20]

The strong dependence of the $N\bar{N}$ amplitude on the momentum transfer corresponds to a large radius in coordinate space. This increases the effective nuclear radius in the $\bar{p}$–nucleus interaction compared with that in the nucleon–nucleus interaction [by one and a half times in the case of the nucleus ^{12}C (Ref. 4)]. It is clear that when the wavelength is comparable to the scatterer size a significant increase of the scatterer size improves the conditions for the optical approximation.

Another possible reason for the smallness of noneikonal corrections is, according to Ref. 71, the strong absorption of the antiproton in the nucleus.

In the Glauber–Sitenko approximation one includes graphs in which the incident particle can scatter on a nucleon of the nucleus no more than one time, that is, the maximum multiplicity of particle scattering in the nucleus is A. In the case of the deuteron this is the double-scattering graph (Fig. 4). A deviation of the antinucleon trajectory from a straight line and the motion of the intranuclear nucleons can lead to multiple-scattering effects. The corresponding graph for scattering on a deuteron is shown in Fig. 5. It is estimated[12,21] that the contribution of n-fold rescattering ($n > 2$) relative to the double-scattering amplitude at low momentum transfers is proportional to $(\sigma_{el}/\sigma_{tot})^{n-2}$. For antinucleons of momentum 300 MeV/c, we have $\sigma_{el}/\sigma_{tot} \approx 1/3$, which can lead to a sizable correction in scattering on a deuteron. Nevertheless, the use of the Glauber–Sitenko theory for $\bar{p}d$ scattering at low and intermediate energies has led to good results[22,23] (other aspects of $\bar{p}N$ and $\bar{p}A$ interactions are also discussed in the reviews of Refs. 23 and 63).

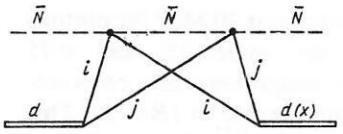

FIG. 4. Graph for double scattering on the deuteron.

b) Cancellation of nonadiabatic and off-shell effects. In the Introduction we have noted that the Glauber–Sitenko theory for hadron scattering on nuclei is to a considerable degree based on the so-called adiabatic approximation. This approximation corresponds to the picture in which the incident particle interacts with a set of free, stationary, "frozen" nucleons. One then averages over all possible positions of the nucleons using the wave functions of the initial and final nuclear states. In terms of the optical analogy, the picture is that of x-ray diffraction on a slowly vibrating crystal lattice.

The surprise here is that the calculations carried out in the adiabatic approximation give a good description of the experimental data in a region which would seem to be far from that where this approximation is applicable, for example, at large momentum transfers. In the case of x-ray diffraction it is as if the lattice parameter varied with a frequency close to that of the incident radiation, but the diffraction picture still remained valid. This larger-than-expected region of applicability has until recently not been understood, since there are relatively large effects which are not included in these schemes. These are: a) the nucleons in the nucleus are not stationary, but they move and are exchanged in the interaction with the incident particle, whose propagation function is changed accordingly; b) the particles inside the nucleus are virtual, that is, the relation between their energy and momentum is not the same as that of a free particle. Because of this the amplitudes of elementary events must be computed off the mass shell; c) during the passage of the incident particle through the nucleus the intranuclear nucleons can rescatter on each other, which also significantly changes the physical picture compared to the adiabatic one.

There are many studies in the literature devoted to the more or less exact inclusion of each of these effects. The result was not very comforting: the inclusion of each of these corrections separately only worsened the agreement with experiment. The natural conclusion is that the success of the

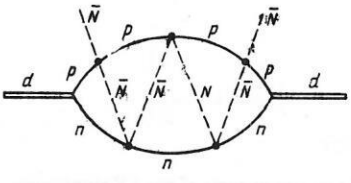

FIG. 5. Graph corresponding to multiple rescattering of the incident particle on the nucleons in the deuteron.

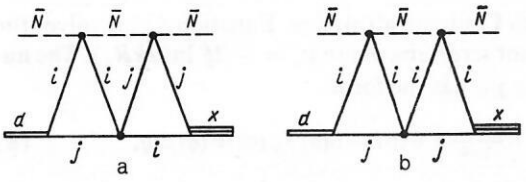

FIG. 6. Graphs describing the rescattering of intranuclear nucleons on each other between scatterings of the initial hadron (antinucleon) on them: a) scattering of the hadron on different nucleons; b) scattering of the hadron on the same nucleon.

simple physical picture of the interaction of the incident hadron with free, stationary nucleons is related to the cancellation of the corrections from these effects. At first glance this cancellation seems impossible or, at least, accidental because of the different physics behind the different corrections. However, a closer study reveals the presence of fairly clear physical relations between these effects based on a relation analogous to the Ward identity in quantum electrodynamics.

The possible reasons for the cancellation of the nonadiabatic and off-shell effects have been studied in detail for the simplest example, that of hadron elastic scattering on deuterons.[8] The Feynman graphs corresponding to single and double scattering of the incident hadron on the nucleons of the deuteron were studied for this purpose. The graph in Fig. 4 corresponds to the Glauber or "shadow" correction to hadron scattering on a deuteron. The graphs in Fig. 6 describe this process when the incident hadron successively scatters on different nucleons (Fig. 6a, where the indices i and j denote nucleons) or the same nucleons in the deuteron (Fig. 6b). The Feynman graphs shown in Figs. 4, 6, and 7 exhaust all the possibilities for single and double scattering.

For comparing the nonadiabatic corrections, it is necessary, first of all, in the graphs of Fig. 6 to exclude the "extra" np scattering, after expressing the amplitude for this scattering in terms of the deuteron vertex function. This is done using the integral relation between the off-shell np scattering amplitude $t(\mathbf{p}, \mathbf{k}, E)$ and the vertex function $M_d(\mathbf{k})$:

$$\frac{M_d(\mathbf{k})}{\varepsilon_d + E} = -\int d^3p \frac{\varphi_d(\mathbf{p})\, t(\mathbf{p}, \mathbf{k}, E)}{E - \frac{\mathbf{p}^2}{m} + i0}, \qquad (1)$$

where $M_d(\mathbf{k}) = (\mathbf{k}^2/m + \varepsilon_d)\varphi_d(\mathbf{k})$, $\varphi_d(\mathbf{k})$ is the deuteron wave function in momentum space, and $\mathbf{k}$ is the relative momentum of the nucleons in the deuteron. A relation of this type is similar in meaning to the familiar Ward identity in quantum electrodynamics. We shall now qualitatively discuss the result of this comparison[8] without writing out the awkward formulas corresponding to the explicit form of the graphs in Figs. 4 and 6. We use ΔM to denote the difference between the exact expression for the Glauber graph (Fig. 4) and the expression obtained in the adiabatic limit, that is, assuming that the nucleons are at rest. The quantity ΔM also directly corresponds to the nonadiabatic correction to the graph in Fig. 4. We add ΔM to the exact expression for the graph in Fig. 6a. Using the relation (1) in Ref. 8, it has been shown that this sum is close to zero. Therefore, the nonadiabatic correction to the Glauber graph (Fig. 4) cancels with the contribution of the graph in Fig. 6a describing the process in which between successive rescatterings of the hadron on different nucleons of the deuteron these nucleons rescatter on each other. The accuracy of this cancellation at small momentum transfers q is of the order of several percent. As the momentum transfer increases the parameter characterizing the degree of cancellation becomes equal to $(1/8)(qR)^2$, where R is the deuteron radius.

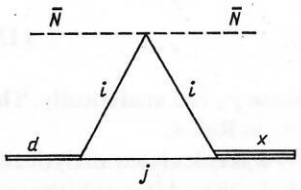

FIG. 7. Graph for single scattering.

Let us now consider the other graphs in Figs. 6b and 7. Since the nucleon in the nucleus is bound, the corresponding hadron–nucleon scattering amplitudes are off-shell (we recall that the Glauber–Sitenko theory always involves the scattering amplitudes on the free nucleon). Nevertheless, it can be shown[8] that the amplitude corresponding to the sum of the graphs in Figs. 6b and 7 is close to the amplitude for single scattering (Fig. 7), but with the elementary amplitude taken at the energy corresponding to scattering on the free nucleon. A similar result has been obtained in Ref. 67. Therefore, there is cancellation of the effect related to departure of the hadron–nucleon scattering amplitude from the mass shell and the rescattering of nucleons between successive hadron scatterings on the same nucleon in the deuteron. The level of this cancellation is the same as in the case of nonadiabatic corrections.

Therefore, the scattering of a hadron on a deuteron in the single- and double-scattering approximation looks as though the hadron had scattered on a stationary nucleon and the scattering amplitude were off-shell. This result generalizes both to the case of inelastic scattering (with deuteron breakup) and to the case where rescatterings of higher multiplicity are included.[8]

The eikonal, Fresnel, and nonadiabatic corrections for the case of complex nuclei have been studied in Ref. 16 using the potential model. All of these corrections turn out to be of the same size. It has also been shown that if for the elementary amplitudes one uses the exact amplitudes, for example, those extracted from the experimental data (as is done in practice), rather than the amplitudes calculated in the eikonal approximation, then the part of the corrections containing the term $1/k$ is thereby taken into account, so that the conditions for the applicability of the Glauber–Sitenko approach are worsened. On the other hand, it has been shown in Ref. 67 that the cancellation between off-shell effects and the rescattering contribution can be violated for $A \gtrsim 3$.

Up to now there has been no detailed study similar to Ref. 8 of the cancellation of different corrections for hadron scattering on complex nuclei. Therefore, the results presented above for hadron–deuteron scattering can be viewed only as an indication (although quite a convincing one) that the adiabatic approximation might be applicable in the scattering of slow antiprotons on complex nuclei. More precise statements about the degree of cancellation of nonadiabatic and off-shell effects can at present be made only on the basis of

comparison with the experimental data. We again stress the fact that the scattering of low-energy antiprotons on nuclei is a unique process in this context, owing to the fact that the requirements of the eikonal approximation and the conditions for cancellation are satisfied independently.

2. ELASTIC SCATTERING

In the studies of Glauber[2] and Sitenko[3] a formula was obtained for the amplitude of the scattering of a hadron on a nucleus A with the transition of the nucleus from the state i to the state f, which expresses the amplitude in terms of the hadron–nucleon scattering phases and the nuclear wave functions:

$$F_{if} = \mathrm{i}\frac{k}{2\pi}\int d^2b \exp(-\mathrm{iqb}) \int d\tau \varphi_f^*(\mathbf{r}_1, \ldots, \mathbf{r}_A) \times \left(1-\exp\left(2\mathrm{i}\sum_1^A \eta_k(\mathbf{b}_k-\mathbf{b})\right)\right)\varphi_i(\mathbf{r}_1 \ldots, r_A). \quad (2)$$

Here $\eta_k(\mathbf{b})$ is the phase of hadron scattering on the kth nucleon in the impact-parameter representation, ψ_i and ψ_f are the nuclear wave functions, and τ are the nucleon coordinates. This formula is the starting point for obtaining the approximate expressions used in numerical calculations of both elastic and inelastic scattering.

The scattering of low-energy antiprotons on nuclei discussed below is unique in that Coulomb effects, which play an important role in the cross section at the diffraction minima and at small angles, are very important in the region where the Glauber–Sitenko approximation is valid. In contrast to high-energy hadron scattering on nuclei, where Coulomb effects lead to small corrections, in $\bar{p}A$ scattering at low energies this effect is significant even for light nuclei. In the Glauber–Sitenko approach Coulomb effects are taken into account by adding a Coulomb phase to the nuclear scattering phase. It is assumed that the nuclear wave function in (2) factorizes. This enables us to abandon multiparticle nuclear wave functions in favor of a simpler object—the nuclear density. After some transformations the amplitude (2) for elastic scattering on a nucleus A taking into account Coulomb effects can be written as[2,17]

$$\exp(\mathrm{i}\chi_s) F_{\mathrm{el}}(q) = F_c(q) + \mathrm{i}k\int_0^\infty J_0(qb)\exp(\mathrm{i}\chi_0(b)) \times [1-\exp(\mathrm{i}(\chi_N(b) + \chi_1(b)))]\, bdb, \quad (3)$$

where

$$F_c(q) = -2\xi\frac{k}{q^2}\exp(\mathrm{i}\varphi_c); \quad (4)$$

$$\varphi_c = -2\xi\ln\left(\frac{q}{2k}\right) + 2\eta, \quad \eta = \arg\Gamma(1+\mathrm{i}\xi); \quad (5)$$

$$\chi_0(b) = 2\xi\ln(kb); \quad (6)$$

$$\chi_1(b) = 8\pi\xi\int_b^\infty \rho(r)\left\{\ln\left[\frac{1+(1-b^2/r^2)^{1/2}}{b/r}\right] - (1-b^2/r^2)^{1/2}\right\} r^2\, dr, \quad (7)$$

where the Coulomb phase is $\chi_c = \chi_0 + \chi_1$ and $J_0(qb)$ is the Bessel function. The parameter ξ in Eqs. (3)–(6) is $\xi = -Z\alpha m/k$, where Z is the nuclear charge and $\alpha = e^2/\hbar c = 1/137$. The minus sign in the formula for ξ corresponds to Coulomb attraction. Equation (3) involves the unimportant screening phase $\chi_s = -2\xi\ln(2kR_s)$. The nuclear phase χ_N has the form[2]

$$\chi_N(b) = \frac{A}{2\pi k}\int \exp(-\mathrm{iqb})\, f_N(q)\,\Phi(q)\, d^2q, \quad (8)$$

where

$$\Phi(\mathbf{q}) = \int \rho(r)\exp(\mathrm{iqr})\, d^3q, \quad (9)$$

$\mathbf{q}$ is the momentum transferred to the nucleus, k is the incident-hadron momentum, and $\rho(r)$ is the nuclear density (normalized to 1). We assume that the charge density $\rho(r)$ entering into (7) coincides with the nuclear density. The amplitude for scattering on a nucleon is

$$f_N(q) = \frac{k\sigma(\mathrm{i}+\varepsilon)}{4\pi}\exp\left(-\frac{1}{2}Bq^2\right). \quad (10)$$

We have used the following parameters of the $\bar{p}N$ amplitudes at the energy $T_{\bar{p}} = 46.8$ MeV (Ref. 24): $\sigma_{\bar{p}p} = 240$ mb, $\sigma_{\bar{p}n} = 200$ mb, $\varepsilon_{\bar{p}p} = \varepsilon_{\bar{p}n} = 0$, $B_{\bar{p}p} = B_{\bar{p}n} = 35.6$ $(\mathrm{GeV}/c)^{-2} = 1.4\,\mathrm{F}^2$. We found the value of $\sigma_{\bar{p}n}$ starting from $\sigma_{\bar{p}d} = 380$ mb (Ref. 25) and taking into account corrections for screening. In Eq. (8) we have made the necessary changes related to the difference between the amplitudes for scattering on a proton and a neutron. These amount to defining the phase $\chi_N(b)$ as the half-sum of the expressions (8) with the $\bar{p}p$ and $\bar{p}n$ amplitudes.

The parameters of the $\bar{p}N$ amplitudes at the energy 180 MeV are the following[5,24]: $\sigma_{\bar{p}p} = 157$ mb, $\sigma_{\bar{p}n} = 136$ mb, $\varepsilon_{\bar{p}p} = \varepsilon_{\bar{p}n} = 0.2$, $B_{\bar{p}p} = B_{\bar{p}n} = 22.2$ $(\mathrm{GeV}/c)^2 = 0.86\,\mathrm{F}^2$.

The nuclear density for $4 \leqslant A \leqslant 16$ is parametrized in the form[26]

$$\rho(r) = [AR^3\pi^{3/2}]^{-1}\left[4 + \frac{2}{3}(A-4)\left(\frac{r}{R}\right)^2\right]\mathrm{e}^{-\frac{r^2}{R^2}}, \quad (11)$$

where $R^2 = 2.50\,\mathrm{F}^2$ for ^{12}C and $R^2 = 2.92\,\mathrm{F}^2$ for ^{16}O (Ref. 26). The phase $\chi_N(b)$ is calculated analytically using the parametrization (11). For heavier nuclei the density is given by the Woods–Saxon formula:

$$\rho(r) = \frac{\rho_0}{1+\exp\left(\frac{r-R}{\tau}\right)}, \quad (12)$$

where $R = r_0A^{1/3}$, $r_0 = 1.07$ F, $\tau = 0.545$ F (Ref. 27), $\rho_0 = 7.675\cdot10^{-3}\ \mathrm{F}^{-3}$ for ^{20}Ne, $\rho_0 = 4\cdot10^{-3}\ \mathrm{F}^{-3}$ for ^{40}Ca, and $\rho_0 = 0.8732\cdot10^{-3}\ \mathrm{F}^{-3}$ for ^{208}Pb.

When the density (12) is used it is impossible to compute the phase $\chi_N(b)$ analytically, and the numerical calculation is more complicated than in the case of high-energy hadron scattering, because the presence of the large parameter B in (10) makes it impossible to move the amplitude $f_N(q)$ in front of the integral sign in (8). We have calculated the phase $\chi_N(b)$ by two methods.

1. We approximated the density (12) by the formula

$$\rho(r) = \sum_{n=1}^{12} c_n \exp(-nr^2/r_a^2), \quad (13)$$

which is used to calculate the phase $\chi_N(b)$ analytically. The parameters in Eq. (13) are given in Ref. 4.

2. The form factor $\Phi(\mathbf{q})$ (9) was calculated analytically using the density (12) (see Ref. 28). After substituting $\Phi(\mathbf{q})$ in (8), the phase $\chi_N(b)$ was found numerically.

The nuclear recoil was taken into account by multiplying the amplitude by the factor $\exp(-\langle r^2\rangle q^2/6A)$ (Ref. 17).

We note that when Coulomb effects are neglected the elastic scattering amplitude has the form

$$F_{\rm el}(q) = ik\int_0^\infty \Gamma(b)\, J_0(qb)\, bdb, \qquad (14)$$

where

$$\Gamma(b) = 1 - \exp(i\chi_N(b)). \qquad (15)$$

The calculated cross sections given below are very sensitive to the parameters of the $\bar{p}N$ amplitude (10), especially to the ratio ε of the real and imaginary parts. At present the uncertainties in the value of ε are very large, and the data of different groups contradict each other. This is seen from the summary of the data given in Fig. 3. In our calculations we shall use the value of ε obtained in the LEAR experiment, but for comparison we give the results of calculations using the value of ε from Ref. 29.

The cross sections for the elastic scattering of antiprotons on the nuclei ^{12}C, ^{40}Ca, and ^{208}Pb at the energies 46.8 and 47.8 MeV are compared with the data[1] in Figs. 8–10. The solid lines correspond to the calculation taking into account Coulomb scattering at $\varepsilon = 0$ (the LEAR value[24]; see Fig. 3). To illustrate the Coulomb scattering, the dot–dash lines in Figs. 8–10 show the Coulomb cross section for scattering on a point charge [the squared modulus of the amplitude (4)]. The dotted line shows the cross section for $\varepsilon = 0$ neglecting Coulomb scattering. At the minimum of the cross section in Fig. 8 and at the second minimum in Fig. 9 the dotted line practically coincides with the dashed line. The dashed lines show the cross sections for $\varepsilon = -0.25$ (Ref. 29). The diffraction minima tend to disappear at $\varepsilon = 0$ and become extremely deep at $\varepsilon = -0.25$, owing to Coulomb–nuclear interference, and the cross sections are very sensitive to the value of ε (except in the case of the nucleus ^{208}Pb, where the dominating role of the Coulomb effects weakens the sensitivity of the cross section to ε). The strong sensitiv-

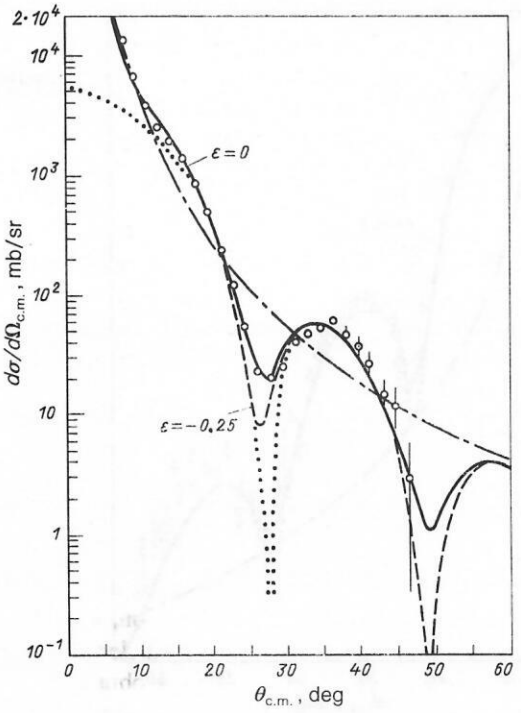

FIG. 9. Differential cross section for $\bar{p}^{40}$Ca elastic scattering at 46.8 MeV. The notation is the same as in Fig. 8.

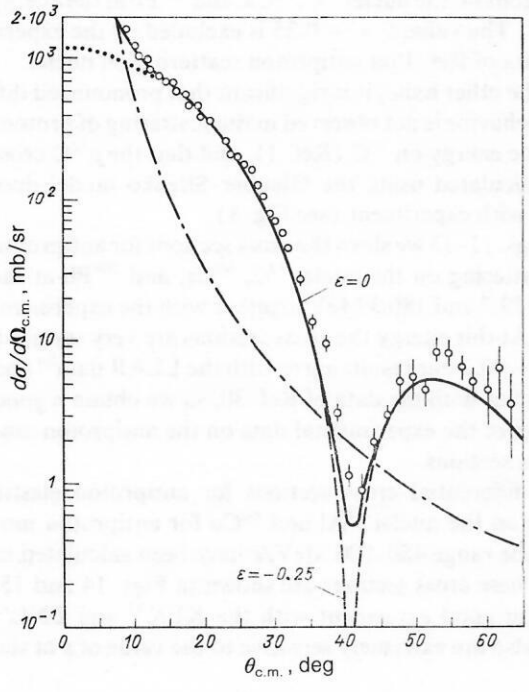

FIG. 8. Differential cross section for $\bar{p}^{12}$C elastic scattering at 46.8 MeV. The solid line corresponds to $\varepsilon = 0$, the dashed line to $\varepsilon = -0.25$, the dotted line to purely nuclear scattering, and the dot–dash line to Coulomb scattering on a point charge Ze. The data are from Ref. 1, and the curves are from Ref. 4.

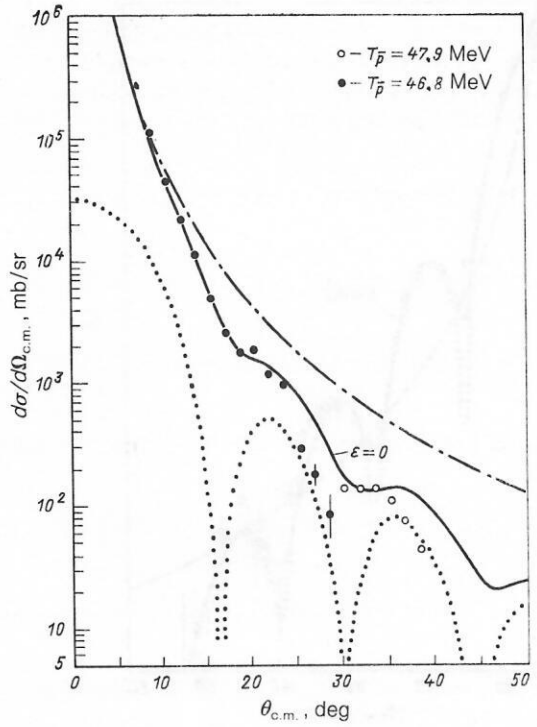

FIG. 10. Differential cross section for $\bar{p}^{208}$Pb elastic scattering. The notation is the same as in Fig. 8.

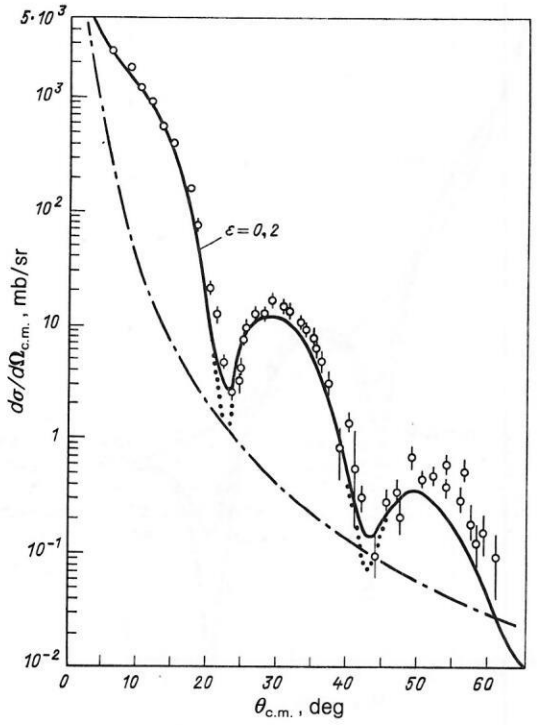

FIG. 11. Differential cross section for $\bar{p}^{12}$C elastic scattering at 179.7 MeV ($\varepsilon = 0.2$). The notation is the same as in Fig. 8.

ity of the cross section to ε arises from the fact that in the absence of Coulomb scattering the cross section is proportional to ε^2 at the diffraction minima (Ref. 4).[2)] When Coulomb–nuclear interference is present, the ε dependence of the cross section at the minima becomes more complicated,

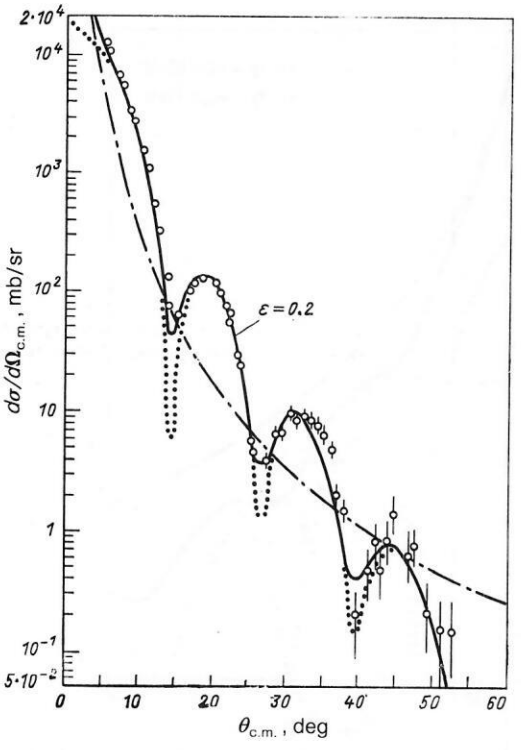

FIG. 12. Differential cross section for $\bar{p}^{40}$Ca elastic scattering at 179.7 MeV. The notation is the same as in Fig. 8.

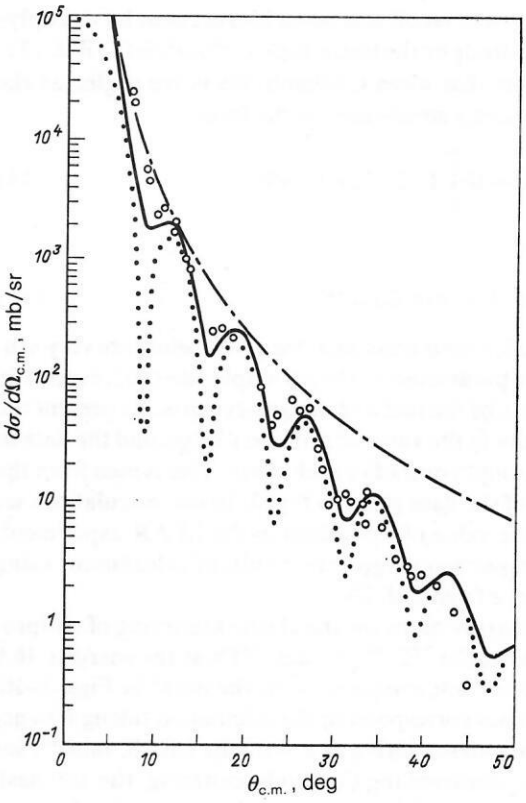

FIG. 13. Differential cross section for $\bar{p}^{208}$Pb elastic scattering at 180.3 MeV. The notation is the same as in Fig. 8.

but, as before, it remains very strong, with the cross section becoming sensitive to the sign of ε. This fact has been pointed out earlier in Ref. 17.

Therefore, at $\varepsilon = 0$ we obtain a good description of the cross sections on the nuclei ^{12}C, ^{40}Ca, and ^{208}Pb at the energy 46.8 MeV. The value $\varepsilon = -0.25$ is excluded by the experimental data of Ref. 1 on antiproton scattering on nuclei.

On the other hand, it is significant that pronounced diffraction behavior is not observed in the scattering of protons of the same energy on ^{12}C (Ref. 1), and that the p^{12}C cross section calculated using the Glauber–Sitenko model does not agree with experiment (see Fig. 1).

In Figs. 11–13 we show the cross sections for antiproton elastic scattering on the nuclei ^{12}C, ^{40}Ca, and ^{208}Pb at the energies 179.7 and 180.3 MeV together with the experimental data.[1] At this energy the cross sections are very sensitive to ε. For $\varepsilon = 0.2$ our results agree with the LEAR data[24] and are consistent with the data of Ref. 30, so we obtain a good description of the experimental data on the antiproton–nucleus cross sections.

The differential cross sections for antiproton elastic scattering on the nuclei ^{27}Al and ^{64}Cu for antiproton momenta in the range 450–900 MeV/c have been calculated in Ref. 28. These cross sections are shown in Figs. 14 and 15. They are in good agreement with the KEK[31] and BNL[32] data and also are extremely sensitive to the value of ε at the minima.

It should, however, be noted that the values of the cross sections at the minima might be sensitive not only to ε, but also to the corrections to the Glauber–Sitenko approximation and also, according to Ref. 33, to the $\bar{p}N$ amplitude with

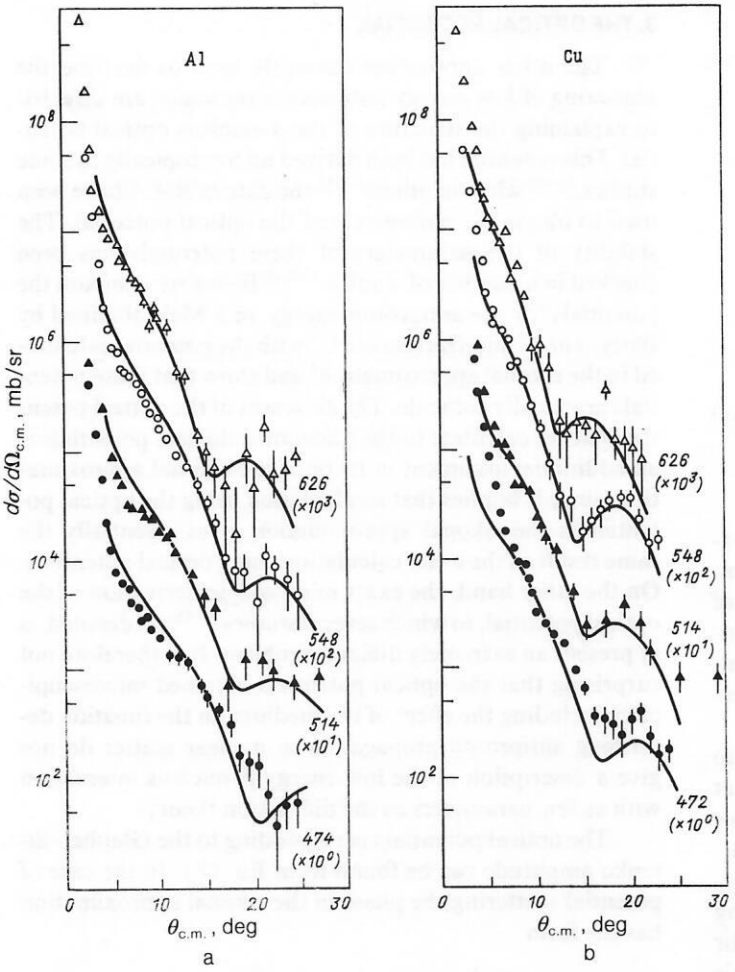

FIG. 14. Differential cross sections for $\bar{p}^{27}$Al and $\bar{p}^{64}$Cu elastic scattering at the antiproton momenta (in MeV/c) shown in the figure. The calculated curves (solid lines) are from Ref. 28. The data at the momentum 514 MeV/c are from Ref. 32, and the data at the other momenta are from Ref. 31.

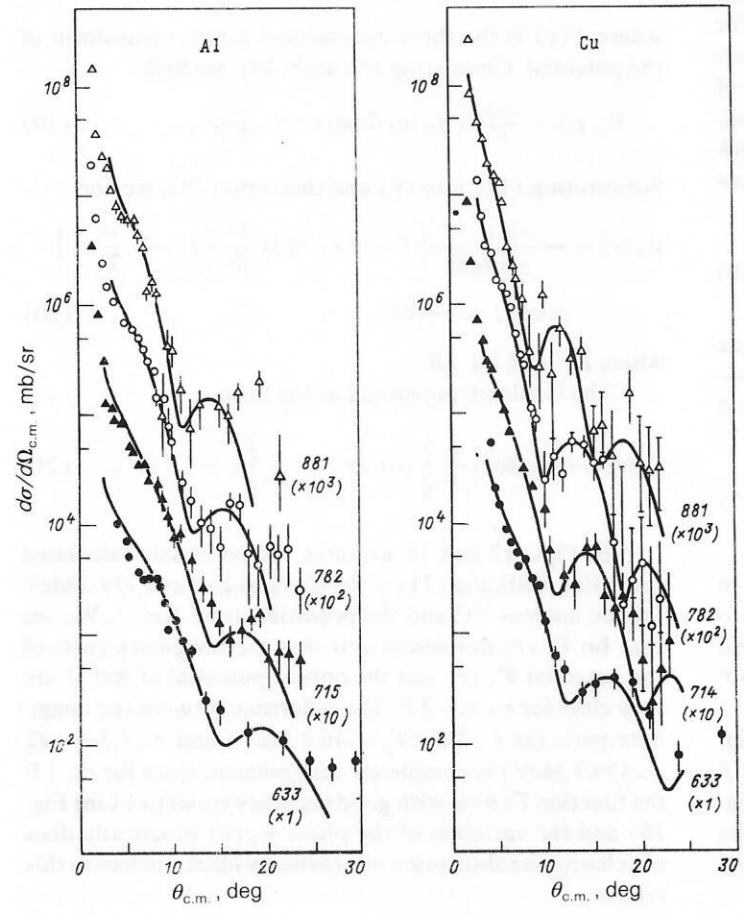

FIG. 15. The same as in Fig. 14. The data at the momentum 633 MeV/c are from Ref. 32, and those at the other momenta are from Ref. 31.

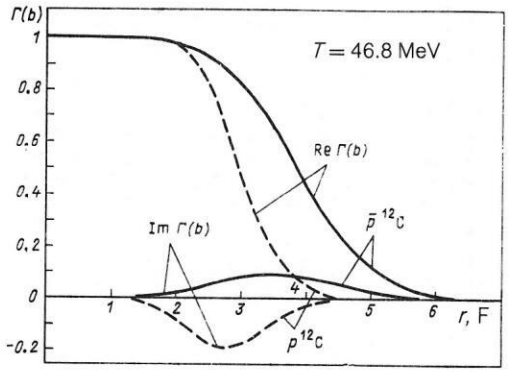

FIG. 16. The profile function $\Gamma(b)$ [see Eq. (15)] for $\bar{p}^{12}C$ (solid lines) and $p^{12}C$ (dashed lines) scattering.

spin flip. Therefore, the accuracy with which ε can be extracted from nuclear data must be determined by independent study of the values of these corrections. The solution of this problem might be aided by the recent data on the antiproton polarization in $\bar{p}A$ scattering[34] and also by a comparative analysis of the cross sections for antiproton scattering on the nuclei ^{16}O and ^{18}O measured in Ref. 35.

Therefore, the use of nuclear data makes it possible to decrease the uncertainty existing in the determination of ε at low energies. It is clear that when the antiproton–nucleus data are included there is a preference for the LEAR data.

In Fig. 16 we show the function $\Gamma(b)$, which determines the amplitude of purely nuclear scattering according to Eq. (14). It is nearly equal to unity inside the nucleus for both antinucleon and nucleon scattering (see Ref. 4). This means that to these particles the nucleus is a perfectly black (in the central region) sphere with a fuzzy boundary. For this reason our calculation of the antiproton–nucleus interaction cross section does not depend on the spin structure of the $\bar{p}N$ amplitude (10), which is important in $\bar{p}p$ scattering.

Let us find the effective radius R_{ef} of a perfectly black sphere. We determine it from the condition that the cross section for scattering on a black sphere of radius R_{ef}

$$\frac{d\sigma}{d\Omega} = \frac{k^2 R_{ef}^2}{q^2} J_1^2(qR_{ef}) \tag{16}$$

coincide at $\theta = 0$ with the squared modulus of the amplitude (14). We note that for Eq. (16) and the Glauber approximation to be valid, we must have $kR_{ef} \gg 1$. From Eqs. (14) and (16) we find

$$R_{ef}^2 = 2\left|\int_0^\infty \Gamma(b)\, bdb\right|. \tag{17}$$

For $\bar{p}^{12}C$ we obtain $R_{ef} = 3.96$ F, which corresponds to the coefficient r_0 in the formula $R = r_0 A^{1/3}$ being equal to 1.73 F, compared with the accepted value $r_0 = 1.07$ F and $R = 1.07 \cdot 12^{1/3} = 2.45$ F. For $p^{12}C$ scattering, $R_{ef} = 3.06$ F (Ref. 4).

We also note that the black-sphere model [see Eq. (16)] gives a good reproduction of the cross section for $\bar{p}$ scattering on ^{12}C up to the first minimum, $q \lesssim F^{-1}$ (see Fig. 1). The calculated value is larger than the experimental one for $q > 1\ F^{-1}$, owing to the enhancement of diffraction by the sharp boundary.

3. THE OPTICAL POTENTIAL

The other approaches currently used to describe the scattering of low-energy antiprotons on nuclei are directed to explaining the structure of the $\bar{p}$–nucleus optical potential. This potential has been derived microscopically in some studies,[36–38] while in others[39–42] the data of Ref. 1 have been used to obtain the parameters of the optical potential. The stability of the parameters of these potentials has been checked in a number of studies.[1,39,40] Below we compare the potentials for the antiproton energy 46.8 MeV obtained by Batty *et al.*,[39] and Garreta *et al.*,[1] with the potential calculated in the eikonal approximation[4] and show that these potentials practically coincide. The closeness of the optical potential that we calculate to the phenomenological potentials is an additional argument in favor of the eikonal approximation, since it implies that a calculation using the optical potential in the eikonal approximation gives essentially the same result as the exact calculation using optical potentials. On the other hand, the exact microscopic derivation of the optical potential, to which several studies[36–48] are devoted, is at present an extremely difficult problem. It is therefore not surprising that the optical potentials obtained microscopically including the effect of the medium on the function describing antiproton propagation in nuclear matter do not give a description of the low-energy $\bar{p}$–nucleus interaction with as few parameters as the diffraction theory.

The optical potential corresponding to the Glauber–Sitenko amplitude can be found from Eq. (8). In the case of potential scattering the phase in the eikonal approximation has the form

$$\chi(b) = -\frac{m}{k}\int V(q) \exp(-iqb)\frac{d^2q}{(2\pi)^2}, \tag{18}$$

where $V(q)$ is the three-dimensional Fourier transform of the potential. Comparing (8) and (18), we find

$$V_N(r) = \frac{2\pi A}{k}\int f_N(q)\,\Phi(\mathbf{q})\, e^{-i\mathbf{qr}}\frac{d^3q}{(2\pi)^3}. \tag{19}$$

Substituting (11) into (9) and then into (19), we find

$$V_N(r) = -\frac{Ak\sigma(i+\varepsilon)}{2\pi^{3/2} m \widetilde{R}^3}\left[1-(1-4/A)\frac{R^2}{\widetilde{R}^2}\left(1-\frac{2}{3}\frac{r^2}{\widetilde{R}^2}\right)\right] \times \exp(-r^2/\widetilde{R}^2), \tag{20}$$

where $\widetilde{R}^2 = R^2 + 2B$.

The Coulomb potential has the form

$$V_c(r) = -4\pi Ze^2\left(\frac{1}{r}\int_0^r \rho(r')\, r'^2\, dr' + \int_r^\infty \rho(r')\, r'\, dr'\right). \tag{21}$$

In Figs. 17 and 18 we show the potentials calculated using Eqs. (20) and (21) at the energies 46.8 and 179.3 MeV for the nucleus ^{12}C and the potentials from Ref. 1. We see that Im $V_N(r)$ dominates and that the imaginary parts of the potential $V_N(r)$ and the optical potential of Ref. 1 are very close for $r > 1.5$–2 F. The difference between the imaginary parts for $r < 2$ F ($T_{\bar{p}} = 46.8$ MeV) and $r < 1.5$ F ($T_{\bar{p}} = 179.7$ MeV) is completely insignificant, since for $r < 2$ F the function $\Gamma(b)$ is with good accuracy equal to 1 (see Fig. 16) and the variation of the phase $\chi_N(b)$ practically does not change the absorption of a perfectly black nucleus in this region.

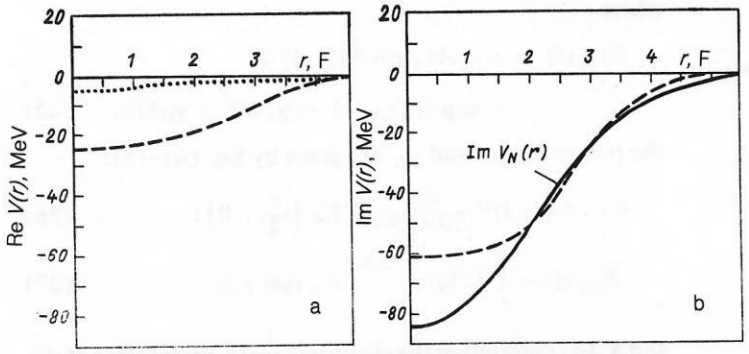

FIG. 17. The optical potential for $\bar{p}^{12}$C scattering at $T_{\bar{p}} = 46.8$ MeV. The solid lines were calculated in Ref. 4 using the theoretical potential corresponding to the Glauber–Sitenko amplitude [calculation using Eq. (20)]. The dashed lines were calculated using the phenomenological potential of Ref. 1 (the Woods–Saxon parametrization). The dotted line shows the Coulomb potential for scattering on the nucleus [Eq. (21)]. Since $\varepsilon = 0$, the solid line in Fig. 17a coincides with the horizontal axis.

Substituting the optical potential (20) together with the Coulomb potential (21) into the Schrödinger equation, we must obtain the same result for the amplitude as in the Glauber–Sitenko approximation (apart from corrections to the eikonal approximation). At the same time, the value and sign of Re $V_N(r)$ are determined by the behavior of ε for the elementary $\bar{p}N$ amplitude, and the radius of the potential is related to the slope parameter in $\bar{p}N$ scattering. It therefore seems to us that the Glauber–Sitenko approach is more attractive, since it gives formulas for the $\bar{p}$–nucleus amplitudes which are clear and convenient for analytical analysis.

We note that the explicit expression for the $\bar{p}$–nucleus potential in the eikonal approximation reveals the reason for the marked enhancement (by a factor of 1.5) of the nuclear radius in antiproton scattering. In Eq. (20), $R_{\text{ef}}^2 \simeq \tilde{R}^2 + 2B$. In the case of low-energy antiprotons, $B \simeq R^2/2$, that is, the slope parameter B is of the order of the squared radius of the nuclear density, which is known from electron scattering. This gives $R_{\text{ef}}^2 \simeq 2R^2$, that is, $R_{\text{ef}} = 1.5R$.

4. THE REACTION CROSS SECTION

The reaction cross section is the difference between the total and elastic cross sections: $\sigma_r = \sigma_{\text{tot}} - \sigma_{\text{el}}$. The total cross section σ_{tot} is expressed by means of the optical theorem in terms of the scattering amplitude at zero angle, while the elastic cross section σ_{el} is obtained by integrating the square of the elastic amplitude over angles. As emphasized above, the Coulomb scattering contribution dominates in the amplitude, especially at small angles. However, this contribution completely drops out of the difference $\sigma_r = \sigma_{\text{tot}} - \sigma_{\text{el}}$. This can be seen from the following formula, obtained in Ref. 3:

$$\sigma_r = \int d^2b \int d\tau \left\{1 - \exp\left(-4 \operatorname{Im} \sum_1^A \eta_k (\mathbf{b}_k - \mathbf{b})\right)\right\} \times |\psi_i(\mathbf{r}_1, \ldots, \mathbf{r}_A)|^2. \quad (22)$$

The Coulomb phase which is added to η_k is real and therefore does not contribute to the reaction cross section (22). After some transformations the reaction cross section takes the form

$$\sigma_r = 2\pi \int_0^\infty [1 - \exp(-2 \operatorname{Im} \chi_N(b))]\, bdb, \quad (23)$$

where the phase $\chi_N(b)$ is given by Eq. (8). Two features should be noted. First, it would be incorrect to attempt to obtain the reaction cross section starting from Eq. (3) for the amplitude. This formula is applicable at angles $\theta > 1/kR_s$, which is more than sufficient for calculations of elastic cross sections, but still does not permit the application of the optical theorem to the amplitude (3). Second, Coulomb scattering has no effect on σ only in the Glauber–Sitenko approximation. When this approximation is not used, Coulomb effects can influence the value of σ_r.

In Fig. 19 we show the reaction cross section for the interaction of antiprotons with the nucleus ^{20}Ne. We see that the calculated cross sections are 10–15% greater than the experimental data.[43] A possible reason for this discrepancy

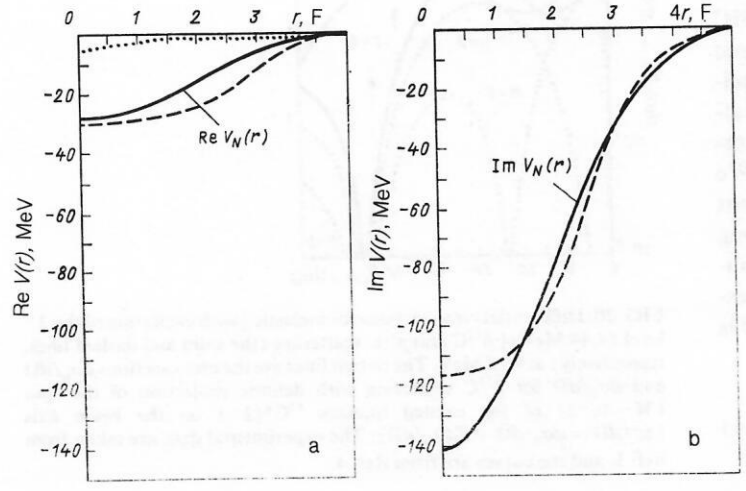

FIG. 18. The optical potential for $\bar{p}^{12}$C scattering at $T_{\bar{p}} = 179.7$ MeV. The notation for the curves is the same as in Fig. 17.

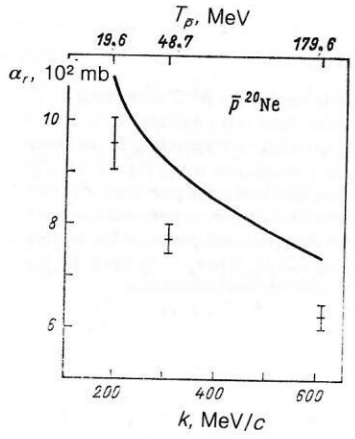

FIG. 19. Reaction cross section for the interaction of antiprotons with the ^{20}Ne nucleus. The calculated curve is from Ref. 28, and the experimental data are from Ref. 43.

is the following. In the calculations it was assumed that the slopes B are identical in $\bar{p}p$ and $\bar{p}n$ scattering. In general this is not so. There are no experimental data on the slope parameter in $\bar{p}n$ scattering, and from the theoretical point of view it seems quite probable that this slope is smaller than in $\bar{p}p$ scattering. The point is that the slope in $\bar{p}p$ scattering is determined by the contribution of $\bar{p}p$ resonances with isospin 0 and 1, while the $\bar{p}n$ system exists only in the state with isospin 1. A 10% decrease of the slope in $\bar{p}n$ scattering would lead to a decrease of the calculated reaction cross section, so that it would agree with the experimental data. We note that this same effect (a decrease of $B_{\bar{p}n}$ relative to $B_{\bar{p}p}$) would cause the minimum of the differential cross section for $\bar{p}A$ scattering to be shifted slightly toward larger $q(\Delta q/q \sim 5\%)$ and would decrease the cross section by roughly 10%, which would lead to better agreement with experiment (see Figs. 8–13).

5. THE CROSS SECTION WITH NUCLEAR LEVEL EXCITATION

The amplitude for scattering with nuclear level excitation is given by Eq. (2) for $i \neq j$. In what follows we shall use the single-inelastic-collision (SIC) approximation,[44,45] in which it is assumed that the level excitation occurs as the result of a single event. After some transformations, the amplitude for inelastic scattering with the excitation of a nuclear level of natural parity with angular momentum J and its projection M on the incident-beam direction in the SIC approximation is expressed in terms of the electromagnetic form factor of the transition and the elastic scattering amplitude. We take into account Coulomb effects in inelastic scattering by including the Coulomb phase in the elastic scattering amplitude entering into the inelastic amplitude. We stress the fact that in this approximation the (single) event causing the level excitation occurs only because of the strong interaction of the incident hadron with an intranuclear nucleon. After the inclusion of Coulomb scattering, the expression for the inelastic amplitude obtained in Refs. 44 and 45 is conveniently written as

$$e^{i\chi_s} F^M_{\text{inel}}(q) = \int_0^\infty G_{JM}(b)\, J_M(qb)\, db, \tag{24}$$

where

$$G_{JM}(b) = C_{JM} A f_N(0)\, \tilde{S}_{JM}(b)\, b \times \exp\{i(\chi_N(b) + \chi_0(b) + \chi_1(b))\}; \tag{25}$$

the phases χ_0, χ_1, and χ_N are given by Eq. (6)–(8);

$$C_{JM} = (-1)^M \frac{2\pi^{1/2}}{(2J+1)^{1/2}} Y^*_{JM}\left(\frac{\pi}{2}, 0\right); \tag{26}$$

$$\tilde{S}_{JM}(b) = \int_0^\infty S_J(q)\, e^{-\frac{1}{2}Bq^2} J_M(qb)\, q\, dq, \tag{27}$$

and $S_J(q)$ determines the electromagnetic form factor of the inelastic transition and is parametrized as

$$S_J(q) = q^J (a_1 + b_1 q^2 + c_1 q^4)\, e^{-\alpha q^2}, \tag{28}$$

which allows the integral (27) to be calculated analytically (see Ref. 4). The parameters in (28) are known from the data on electron inelastic scattering. For the excitation of the 2^+ level (4.44 MeV) of the nucleus ^{12}C we have taken them to be[46] $a_1 = 0.25$, $b_1 = -0.021$, $c_1 = 0.0004$, and $\alpha = 0.54$ [in Eq. (28), q is in F^{-1}].

The calculated inelastic $\bar{p}^{12}$C cross sections with excitation of the 2^+ level (4.44 MeV) are shown in Figs. 20 and 21 for the energies 46.8 and 179.7 MeV, respectively. The antiproton data of Ref. 1 are described satisfactorily (solid lines). However, the calculation (dashed line in Fig. 20) does not agree with the proton data, as in the case of elastic scattering (see Fig. 1).

The slightly higher values of the antiproton data compared with the calculation in Fig. 20 for $\theta > 35°$ ($q > 0.8$ F^{-1}) can be attributed to several factors. In particular: a) the uncertainties in the transition form factor (28); b) the decreased accuracy of the Glauber–Sitenko approximation in large-angle scattering; c) the collective nature of the excited 2^+ level and the inapplicability of the SIC approximation in this case. In connection with possibility (c), we note that the model which takes into account the collective (rotational) nature of the 2^+ level (4.44 MeV) gives a cross section for the inelastic scattering of protons of energy 1 GeV on

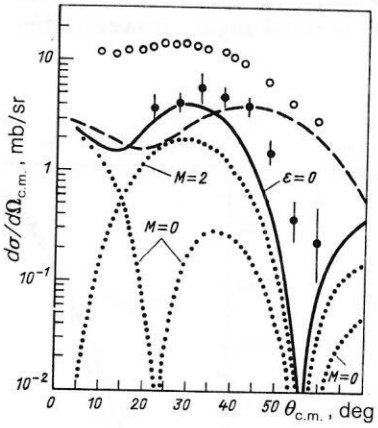

FIG. 20. Differential cross sections for inelastic [with excitation of the 2^+ level (4.44 MeV)] $\bar{p}^{12}$C and p^{12}C scattering (the solid and dashed lines, respectively) at 46.8 MeV. The dotted lines are the cross sections $d\sigma_0/d\Omega$ and $d\sigma_2/d\Omega$ for $\bar{p}^{12}$C scattering with definite projection of the spin ($M = 0$, 2) of the excited nucleus ^{12}C*(2^+) on the beam axis ($d\sigma/d\Omega = d\sigma_0/d\Omega + 2d\sigma_2/d\Omega$). The experimental data are taken from Ref. 1, and the curves are from Ref. 4.

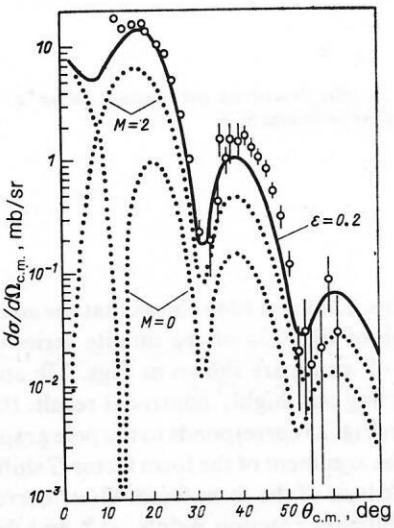

FIG. 21. Differential cross section for inelastic [with excitation of the 2^+ level (4.44 MeV)] $\bar{p}^{12}$C scattering at 179.7 MeV ($\varepsilon = 0.2$). The notation is the same as in Fig. 20.

^{12}C (see Ref. 47) which is larger than that calculated in the shell model[26] and leads to a good description of experiment. A similar increase of the experimental value relative to the calculated value within the framework of the SIC in the region to the right of the maximum has also been observed in the cross section for excitation of a ^{16}O level (3^-, 6.13 MeV) by high-energy π^+ mesons (Ref. 48). This discrepancy vanished in a model which treats the level (3^-, 6.13 MeV) as a rotational level, with the calculation[49] being carried out using the Glauber–Sitenko theory, rather than the SIC approximation (Fig. 22). Such studies of the effect of nuclear structure on the antiproton–nucleus interaction are therefore certainly interesting.

We stress the fact that the level-excitation amplitude is very sensitive to the nuclear surface.[44,45] In fact, the factor $e^{i\chi_N} = 1 - \Gamma(b)$ in Eq. (25) is equal to 0 inside the nucleus and becomes 1 outside it. On the other hand, the function $\tilde{S}(b)$ falls off rapidly outside the nucleus. Therefore the integral (24) is determined by the overlap region near the nuclear surface. The function $G_{JM}(b)$ determining the amplitude (24) is thus nonzero only in the overlap region near the nuclear surface.

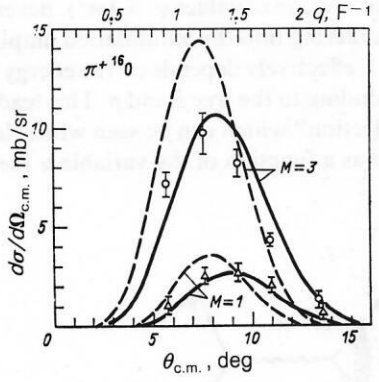

FIG. 22. Differential cross sections for excitation of the 3^- level (6.13 MeV) of the ^{16}O nucleus by pions of momentum 2 GeV/c corresponding to spin projections $M = 1$ and $M = 3$ of the nucleus ^{16}O* (3^-) on the beam direction. The solid lines correspond to the calculation of Ref. 49 using the Glauber–Sitenko formulas,[2,3] and the dashed lines correspond to the calculation in the approximation of a single inelastic collision. The experimental data are from Ref. 48: △ for $M = 1$, ○ for $M = 3$.

We note that the calculation of the level-excitation cross section in the black-sphere model with a sharp edge is very crude and decreases the result by a factor of 2–3.

In Figs. 20 and 21 we also give the predictions for the antiproton cross sections with the projection M of the spin of the excited nucleus on the beam axis equal to 0 and 2:

$$\frac{d\sigma}{d\Omega} = \frac{d\sigma_0}{d\Omega} + 2\frac{d\sigma_2}{d\Omega}$$

according to Eq. (26), $C_{21} = 0$, and therefore $d\sigma_1/d\Omega = 0$. The measurement of these cross sections, which, as seen from the figure, have a very complicated angular dependence, would provide more detailed verification of the theory.

The cross section $d\sigma_M/d\Omega$ can easily be obtained from the angular distributions of photons emitted when the nucleus makes a transition to the ground state. Such experiments for the nucleus ^{16}O in a beam of π^+ mesons and protons at high energy have been carried out in Ref. 48. The photon angular distribution is determined by the polarization density matrix of the excited nucleus:

$$\rho_{MM'}(q) = F^M_{\text{inel}}(q)\, F^{M*}_{\text{inel}}(q) \Big/ \sum_M |F^M_{\text{inel}}(q)|^2. \tag{29}$$

From the expressions (24)–(27) we find

$$\rho_{MM'} = \rho_{-M,-M'}\rho_{M,-M'} = (-1)^M \rho_{M,M'}$$

$$\rho_{-M,M'} = (-1)^M \rho_{MM'}.$$

Therefore, for the level with $J = 2$ the density matrix is determined by only three independent elements: ρ_{00}, ρ_{22}, and ρ_{20} [according to Eq. (26), the amplitude $F^M_{\text{inel}}(q)$ is nonzero only for projections M having the same parity as J]. The angular distribution of photons emitted in the transition $J \to 0$ can be obtained from the formula

$$W(\theta_\gamma, \varphi_\gamma, q) = \sum_{MM'} \rho_{MM'}(q)\, Y^{(\lambda)}_{JM}(\theta_\gamma, \varphi_\gamma)\, Y^{*(\lambda)}_{JM}(\theta_\gamma, \varphi_\gamma), \tag{30}$$

where $\mathbf{Y}^{(\lambda)}_{JM}(\theta_\gamma, \varphi_\gamma)$ are the known spherical vectors of the photon, θ_γ is the angle between the direction of the incident beam and the photon momentum, and φ_γ is the angle between the $(\bar{p},\bar{p}')$ scattering plane and the plane formed by the momenta of the incident beam and the photon. Explicit expressions for the angular distributions of photons emitted in the de-excitation of nuclei with $J = 2$ and $J = 3$ are given in Ref. 4.

6. ANNIHILATION CHANNELS

Up to now we have considered only inelastic reactions in which the scattering of the incident antiproton causes the nucleus to make a transition into one of the low-lying excited states. There are also other interesting inelastic reactions in which the antiproton "disappears" in the nuclear matter because of annihilation with a nucleon of the nucleus. In this case, the reaction products include not only the products of the nucleus breakup, but also states with baryon number equal to zero (systems of several π or K mesons, lepton pairs, and so on). In this process the antiproton annihilation

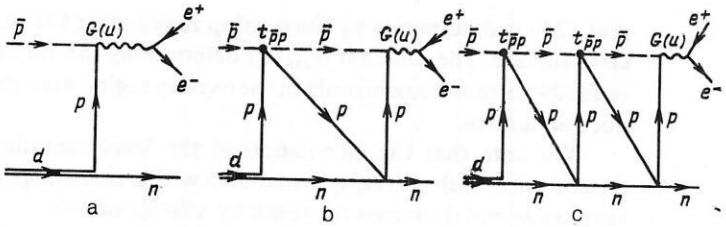

FIG. 23. Graphs describing the reaction $\bar{p}d \to e^+e^- n_s$, neglecting the $\bar{p}n$ interaction.

occurs not on a free nucleon, but on a nucleon bound in the nucleus. It would seem that this makes it possible to obtain information on the amplitude for antiproton–nucleon annihilation in a kinematic region inaccessible to study in reactions with a hydrogen target. However, as we have already noted above, owing to unique cancellations of nonadiabatic and off-shell effects this process occurs as though the incident antiproton were interacting with a free nucleon, that is, an on-shell nucleon. As we shall see below, because of this experiments using nuclear targets cannot give information on the annihilation amplitude in a region inaccessible in free kinematics. However, it does lead to rather curious predictions concerning the annihilation of slow antiprotons in nuclei which can be checked experimentally.

Here we shall consider an example related to the study of the amplitude for lepton pair production in the annihilation of slow antiprotons on deuterium, i.e., the process $\bar{p} + d \to e^+e^- + n_s$ (here n_s is the spectator neutron). This reaction is interesting mainly because knowledge of the amplitude for the elementary process $\bar{p} \ll p \gg \to e^+e^- \ll p \gg$ is the proton bound in the nucleus) is actually equivalent to study of the proton electromagnetic form factor in the unphysical region, that is, for $q^2 < 4m^2$, where q is the four-momentum of the e^+e^- system and m is the nucleon mass.

The amplitude for this process corresponds to the infinite series of graphs in Fig. 23, in which the proton of the deuteron rescatters on the neutron between two successive $\bar{p} \ll p \gg$ rescatterings. The simplest of these—the impulse-approximation graph (the pole graph)—involves the following expression (the amplitude of the virtual process $\bar{p}d \to \gamma^* n$):

$$M_0 = \varphi_d(\mathbf{p}_s)\, G(u). \tag{31}$$

Here $\varphi_d(\mathbf{p}_s)$ is the deuteron wave function, $\mathbf{p}_s$ is the momentum of the spectator neutron, and $G(u)$ is the amplitude of the annihilation $\bar{p} \ll p \gg \to \gamma^*$ at energy u, that is, the form factor. The energy

$$u = \frac{(\mathbf{k}+\mathbf{p}_s)^2}{4m} - \frac{\mathbf{p}_s^2}{m} - \varepsilon_d = v - \frac{\mathbf{p}_s^2}{m} - \varepsilon_d \tag{32}$$

corresponds to $u = \sqrt{q^2} - 2m$, that is, the total energy of the e^+e^- system minus the two nucleon masses (k is the momentum of the incident antiproton), and

$$v = (\mathbf{k} + \mathbf{p}_s)^2/4m, \tag{33}$$

where v is the kinetic energy in the center-of-mass system of the free p and $\bar{p}$, and ε_d is the deuteron binding energy.

By summing the Feynman graphs taking into account intermediate rescatterings, the authors of Refs. 8 and 50 showed that the amplitude of the transition $\bar{p}d \to \gamma^* n$ corresponding to the sum of all the graphs in Fig. 23 will be

$$M = M_0 + M_1 + M_2 + \ldots = \varphi_d(\mathbf{p}_s)\, G(v). \tag{34}$$

Comparison of Eqs. (31) and (34) shows that the addition to the pole graph of Fig. 23a of the infinite series of graphs (the first two of which are shown in Figs. 23b and 23c) leads to a surprising and highly nontrivial result: the sum of all the graphs in Fig. 23 corresponds to the pole graph of Fig. 23a, but with the argument of the form factor G shifted relative to (31). Instead of the form factor $G(u)$ corresponding to the annihilation reaction $\bar{p} \ll p \gg \to \gamma^*$ and depending on the energy u, it is possible to use subthreshold values; as a result, this form factor comes in at the energy v corresponding to annihilation on a free proton. It is as though the inclusion of rescatterings pushes the energy of the $p\bar{p}$ system above threshold. In the derivation of Eq. (34) it is important to use the fact that the $\bar{p}p$ interaction in the initial state, which is determined by the amplitude $\bar{p}p \to e^+e^-$ and the form factor $\bar{p}p \to \gamma^*$ (Fig. 24), is given by the same dynamics as $\bar{p}p$ rescatterings inside the deuteron. The amplitudes $t_{\bar{p}p}$ in Figs. 24 and 23 are the same amplitude.

The order of the corrections to Eq. (34) is determined by the relation $\Delta M \sim \varphi_d(p_s)|G(u) - G(v)|/8$ and, as shown by model calculations,[8] does not exceed 30%. Of course, the corrections to Eq. (34) can complicate this formula and distort the result, but there is no reason to think that they lead to the inverse replacement of the argument v in (34) by the argument u. It should be noted that, as we have seen above in calculations of the cross sections for $\bar{p}$ scattering on nuclei in the Glauber approximation, this sort of cancellation of off-shell effects in practice occurs with very high accuracy.

Let us now discuss the physical consequences of the result which we have obtained. It follows from (34) that, in spite of the fact that the "kinetic energy" of the colliding antiproton and proton in the c.m.s. frame of the particles e^+ and e^-, equal to $u = \sqrt{q^2} - 2m$, can become negative (i.e., we enter the "unphysical" region of values $q^2 \lesssim 4m^2$), nevertheless the form factor entering into the annihilation amplitude $M(\bar{p} \ll p \gg \to e^+e^-)$, effectively depends on the energy v [see Eq. (33)] corresponding to the free $\bar{p}$ and p. This leads to a unique sort of "reflection" which can be seen when the form factor G is plotted as a function of the variable u [see

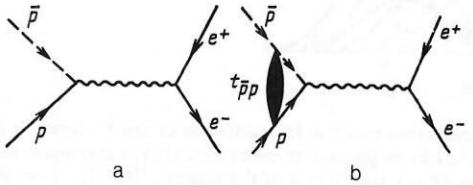

FIG. 24. Graphs describing the annihilation reaction $\bar{p}p \to e^+e^-$, where $t_{\bar{p}p}$ is the elastic $\bar{p}p$ scattering amplitude, which also enters into the graphs of Fig. 23.

Eq. (32)]. This is the dependence which is usually studied, because it is erroneously assumed that the form factor for the argument equal to the energy of the e^+e^- pair, i.e., u, is extracted from the cross section of the reaction $\bar{p}d \to e^+e^-n$. Using Eqs. (32) and (33), it is possible to select the kinematics such that when the variable u falls off monotonically, the variable v does not behave monotonically, for example, first v decreases to zero, then it increases. It is well known that the proton electromagnetic form factor grows as the boundary of the unphysical region is approached, that is, for $q^2 \to 4m^2 + 0$ (which corresponds to $v \to +0$). The nonmonotonic behavior of the variable v will lead to the experimental observation of a peak.

In order to check this prediction it is interesting to carry out the following experiment. First we select events with $\mathbf{p}_s = 0$ and decrease the incident antiproton momentum ($k \to 0$). Then from (33) it is clear that $v \to 0$, while $G(v)$ increases as the $\bar{p}p$ threshold is approached and at $v = 0$ reaches its maximum value (this corresponds to $u = -\varepsilon_d$). Then we must select events with $\mathbf{p}_s > 0$ (here the antiproton momentum should be $\mathbf{k} = 0$). This leads to a decrease of u with increasing $\mathbf{p}_s$ and to an increase of $v = \mathbf{p}_s^2//4m^2$. Since v grows with increasing $\mathbf{p}_s$, the form factor $G(v)$ decreases (in terms of the variable v we are receding from the "unphysical" region). Therefore, a peak appears at $u = -\varepsilon_d$. Under other kinematic conditions this peak can be shifted or can completely disappear. In fact, let us take the minimum value of the incident antiproton momentum $k = k_0$, and assume that the neutrons go off at an angle of 180° to the direction of the incident antiproton in the laboratory frame. Then for sufficiently large k_0 the value $v = (k_0 - p_s)^2/4m$ cannot reach zero, but will only decrease with increasing p_s. Therefore, the value of $G(v)$ will increase, but will not reach the maximum. This picture is illustrated by direct calculations of G, the graph of which as a function of the energy u is shown in Fig. 25. The curve for G at large values $v \geqslant 0$ (in the physical region $q^2 \geqslant 4m^2$) is taken from Ref. 51. In Fig. 25 we clearly see the peak at $u = -\varepsilon_d$. The range of values of the energy u below threshold is quite broad (up to 10 MeV), so it is fully possible that this effect can be observed experimentally. It becomes possible to increase the range of u in the case of lepton pair production in the annihilation of slow $\bar{p}$ on nuclei heavier than deuterium, that is, in processes like $\bar{p}A \to e^+e^- + A$.

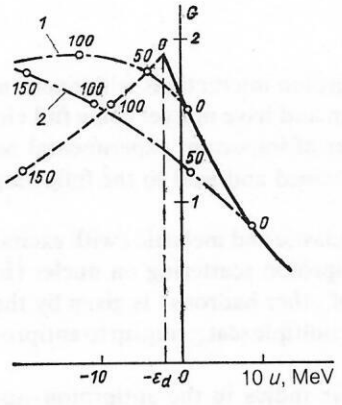

FIG. 25. Behavior of the form factor $G(v) = G(u + p_s^2/m + \varepsilon_d)$ as a function of the variable $u = \sqrt{s} - 2m$, where $\sqrt{s}$ is the effective mass of the e^+e^- system. The solid line corresponds to zero momentum of the spectator neutron ($p_s = 0$), and the dashed line corresponds to annihilation of stopped antiprotons ($k = 0$). [The numbers on the curves give the values of the spectator-neutron momentum in MeV/c. The dot–dash curves labeled 1 and 2 were calculated in the kinematics corresponding to emission of the neutron at an angle of 180° relative to the incident antiproton momentum in the lab frame (the antiproton momentum is 100 and 200 MeV/c for curves 1 and 2, respectively)] (Ref. 8).

TABLE I. Relative yields of ^{3}He nuclei in $\bar{p}^4$He annihilation.

Antiproton kinetic energy $T_{\bar{p}}$, MeV	Cross section for production of the ^{3}He nucleus, $\sigma(^3\text{He})$, mb	Relative yield of ^{3}He, $f(^3\text{He})$
19.6	93.2±7.9	0.136±0.012
48.7	58.6±4.0	0.118±0.008
179.6	35.7±2.8	0.101±0.008

The work scheduled to be carried out at LEAR, which has been discussed above, includes the high-priority study of antiproton annihilation on deuterium with lepton pair production. This means that we shall obtain an answer to the question discussed above in the very near future.

Let us discuss another process, the interaction of $\bar{p}$ with the nuclei ^{4}He and ^{20}Ne. The experiment carried out at LEAR[52,53] measured the total cross sections,[52] the charged-particle multiplicity,[52] and the relative probability of the yield of ^{3}He in the $\bar{p}^4$He interaction,[53] which is of great interest for astrophysics (see Ref. 68 and the reviews of Refs. 54 and 55). The results for the latter process are given in Table I. These data were used to obtain the first estimate of the amount of antimatter in the early universe, which is[53]

$$R = n_{\bar{p}}/n_p < (0.7 - 1.1)\cdot 10^{-3}.$$

The new experimental data on the strange-particle (Λ, $\bar{\Lambda}$, K_S^0) yields in antiproton annihilation on complex nuclei[69] are also very interesting. These yields have turned out to be considerably (several times) larger than in annihilation on the proton (see the review of Ref. 70).

7. SCATTERING LENGTH OF ANTINUCLEONS ON THE NUCLEI ^{12}C AND ^{16}O

The investigation of the nuclear interaction between antiprotons and nuclei at zero energy is directly related to the study of the spectrum and properties of antiprotonic atoms. Owing to the strong interaction, the levels of antiprotonic atoms are shifted and broadened compared to their unperturbed (Coulomb) values. In turn, the shift and width of the levels of the antiprotonic atom (as for any other hadronic atom) are expressed in terms of the partial-wave amplitudes for scattering at zero energy, that is, in terms of the corresponding scattering lengths for the antiproton scattering on the nucleus.

The experimentally observed level shift of the hadronic atom, $\Delta E_{n,l}$, is related to the corresponding hadron–nucleus scattering length as[56]

$$\Delta E_{n,l} = E^c_{n,l}\,\frac{1}{[(2l+1)!!]^2}\,\frac{4}{n}\,a_l\,\frac{1}{r_B^{2l+1}}\prod^{l}\left(\frac{1}{p^2}-\frac{1}{n^2}\right), \quad (35)$$

where l is the orbital angular momentum, n is the principal quantum number, r_B is the radius of the corresponding Bohr

orbit, $E_{n,l}$ is the energy of the unperturbed Coulomb level, and $\Delta E_{n,l} = E_{n,l} - E^c_{n,l}$, where $E_{n,l}$ is the experimental value of the energy level. We note that the "expulsion," that is, the decrease of the absolute value of the binding energy, corresponds to a positive shift $\Delta E_{n,l}$ in this definition.

In the case of the antiprotonic atoms of carbon and oxygen, the measured x-ray spectrum (4f–3d transitions) allows the shift of the 3d level to be determined. According to the experimental data,[3)]

$$E_{3,2} = \begin{cases} (4 \pm 10) \text{ eV} & \text{for } {}^{12}\text{C (data of Ref. 57);} \\ (124 \pm 36) \text{ eV} & \text{for } {}^{16}\text{O (data of Ref. 58).} \end{cases} \quad (36)$$

Using Eq. (35), these values of the shifts can be directly expressed in terms of the scattering lengths $a_2({}^{12}\text{C})$ and $a_2({}^{16}\text{O})$. The method of calculation used in the preceding sections—the Glauber–Sitenko approximation—cannot be used directly to describe antiproton scattering on nuclei at zero energy, that is, for finding the scattering lengths. This can be seen by using Eq. (14) to find the partial-wave amplitudes $f_l(k)$ and formally taking k to zero: we obtain an absurd result—the incorrect behavior $f_l(k) \sim k^{2l+1}$ at small k and vanishing scattering lengths for all the partial waves, since

$$a_l = \lim_{k \to 0} f_l(k)/k^{2l}. \quad (37)$$

However, the results discussed in the preceding sections can still be applied to this case if we make use of the fact that the scattering of low-energy antiprotons on nuclei is described fairly well (at least near the first diffraction minimum) by the model of a perfectly absorbing, black sphere (see Sec. 2 and Fig. 1). On the other hand, the radius of such a sphere can be computed exactly using the Glauber approximation [see Eq. (17)]. If we now assume that the radius of the absorbing sphere is not changed in going to zero energy, the problem reduces to the calculation of the exact amplitude for scattering on a complex potential well

$$V(r) = \begin{cases} V_0 - iW_0, & r \leqslant R_{\text{ef}}; \\ 0, & r > R_{\text{ef}}, \end{cases} \quad (38)$$

where $W_0 > 0$ and after the calculation $a_l W_0$ is taken to infinity. The radius R_{ef} entering into (38) was found in Sec. 2 for the nucleus ${}^{12}\text{C}$ [$R_{\text{ef}}({}^{12}\text{C}) = 3.96$ F]. The same radius for the nucleus ${}^{16}\text{O}$ is $R_{\text{ef}}({}^{16}\text{O}) = 4.31$ F. We note that after calculating the phase (18) in the potential (38) and substituting it into (15) for $W_0 \to \infty$ we obtain the step function $\Gamma(b)$, that is, Eqs. (16) and (17) are reproduced. After computing the phase for scattering in the potential (38), taking W_0 to infinity, expressing the amplitude $f_l(k)$ in terms of the phase, and substituting it into Eq. (37), we find[4]

$$a_l = -\frac{R_{\text{ef}}^{2l+1}}{(2l+1)\,[(2l-1)!!]^2}. \quad (39)$$

We note that if the scattering on the potential (38) gives rise to a complex phase, in the limit of an infinitely deep imaginary well we obtain a real phase and scattering length. A similar phenomenon has been discovered[60] in the coupled-channel model when the constant describing coupling to the inelastic channel is taken to infinity. For $l = 2$ we find $a_2 = -(1/45) R_{\text{ef}}^5$. From this, using the value of R_{ef} we calculate the following values of the d-wave scattering length:

$$a_2({}^{12}C) = -21.7 \text{ F}^5, \quad a_2({}^{16}O) = -33.2 \text{ F}^5. \quad (40)$$

Substitution of these scattering lengths into Eq. (35) leads to the following values for the level shifts:

$$E_{3,2} = \begin{cases} 6.3 \text{ eV} & \text{for } {}^{12}\text{C}; \\ 81.3 \text{ eV} & \text{for } {}^{16}\text{O}. \end{cases} \quad (41)$$

These values are in good agreement with the experimental data on the level shifts quoted above [see (36)].

We stress the fact that the scattering length (39) for $l = 2$ is very sensitive to R_{ef}, which, as noted above, is considerably (more than 1.5 times) greater than the nuclear radius and grows with decreasing energy (owing to the increase of the slope parameter B). The closeness of the experimental values of the level shifts (36) to the theoretical values (41), which involve R_{ef} at the energy 46.8 MeV, can be interpreted as an indication that R_{ef} is saturated at an energy of order 50 MeV and practically stops growing as the energy is increased further. The physical interpretation of this behavior is obvious. At an energy of order 50 MeV the relative momentum of the $\bar{p}$ and "N" reaches values of the order of the intranuclear momenta and remains here as the beam momentum is decreased further. Therefore, even if the slope parameter B in scattering on a stationary nucleon continues to grow with decreasing $T_{\bar{p}}$, this has no effect on scattering on the nucleus.

We therefore see that for finding the scattering lengths and level shifts the Glauber–Sitenko approximation again has certain advantages compared with the phenomenological optical potentials[39,40] generally used to obtain a unified description of the data on low-energy scattering and the level shifts of antiprotonic atoms. Knowledge of the antiproton scattering mechanism makes it possible, without the use of free parameters, to calculate the effective nuclear radius, which is expressed in terms of the parameters of the elementary amplitude and the nuclear density. Then, even where the Glauber–Sitenko approximation is not valid, this radius can be used to calculate the level shifts of antiprotonic atoms.

CONCLUSIONS

Investigations of antiproton interactions with nuclei at LEAR have only just begun and have not yet come full circle. Nevertheless, a number of important experimental results have already been obtained and lead to the following conclusions.

1. The mechanism for elastic and inelastic (with excitation of nuclear levels) antiproton scattering on nuclei (in contrast to the scattering of other hadrons) is given by the Glauber–Sitenko theory of multiple scattering up to antiproton energies $T_{\bar{p}} \simeq 50$ MeV.

2. The effective nuclear radius in the antiproton–nucleus interaction is significantly larger (1.5 times larger in the case of ${}^{12}\text{C}$) than in electron scattering.

3. The cross sections for antiproton–nucleus reactions at the diffraction minima are extremely sensitive to the ratio ε of the real and imaginary parts of the $\bar{p}N$ amplitude. This fact can be used to determine ε from the nuclear data. The antiproton–nucleus cross sections can also be useful for finding other parameters of the $\bar{p}N$ amplitude.

4. The level shifts of the antiprotonic atoms $\bar{p}^{12}C$ and $\bar{p}^{16}O$ are described using the scattering lengths calculated for the effective radius R_{ef} taken at an energy of order 50 MeV. This shows that the effective radius ceases to grow with decreasing energy for $T_{\bar{p}} < 50$ MeV.

5. The ^{3}He nucleus is created roughly 10% of the time in $\bar{p}^4$He interactions. This number puts a limit on the fraction of antiprotons in the early universe relative to the number of protons (the fraction is less than 10^{-3}).

These results pose new problems for theory and experiment.

Among the theoretical problems is that of understanding the reasons for and the true range of validity of the Glauber–Sitenko approximation in the scattering of antiprotons on nuclei at low energy and large angles. We stress the fact that in Ref. 4 we have shown only that the Glauber–Sitenko approximation is valid but have not determined why it is. Of course, when there is agreement between theory and experiment without extensive theoretical justification, the first question that must be answered is that of whether or not this agreement is accidental. In our opinion, the possibility that the agreement in this case is accidental is practically excluded by the combined analysis carried out in Refs. 4 and 28 of the data for the nuclei ^{12}C, ^{20}Ne, ^{27}Al, ^{40}Ca, ^{64}Cu, and ^{208}Pb at various energies. It is now extremely important to obtain a theoretical explanation of the contribution of the corrections to the Glauber–Sitenko mechanism at the diffraction minima, in order to know the degree to which these corrections are responsible for "filling in" these minima and for the ratio of the real and imaginary parts of the elementary amplitude. The surprising fact is the striking cancellation of effects of different physical origin: the correction for the nonadiabatic nature of the nucleon motion in the nucleus and the departure of the elementary amplitudes from the mass shell. In principle, such a cancellation is possible, but the accuracy with which it occurs in the scattering of slow antiprotons greatly exceeds theoretical expectations.

Among the experimental problems is the measurement of the antiproton–nucleus cross sections (preferably for $T_{\bar{p}} < 50$ MeV), in particular, a detailed and accurate measurement in the vicinity of the diffraction minima. Polarization experiments might prove to be very informative. In order to investigate the antiproton–nucleus interaction mechanism in greater detail it is of interest to refine the parameters of the $\bar{p}N$ amplitude (in particular, the ratio of the real and imaginary parts and the slope parameter) in direct experiments on $\bar{p}N$ scattering.

There is a need for more accurate measurements of the cross sections for electron scattering on nuclei with nuclear level excitation for the purpose of finding the transition form factors needed in calculations of the antiproton–nucleus inelastic cross sections.

The early experiments at LEAR have shown that the interaction of low-energy antiprotons with nuclei represents a vital, rapidly developing field of research which promises new and unexpected results.

The authors are grateful to I. S. Shapiro for useful and stimulating discussions.

[1)] The pN scattering amplitude has an exponential dependence on the square of the momentum transfer q^2 [$\sim\exp(-\frac{1}{2}Bq^2)$], and the parameter B in the exponent is referred to as the slope parameter [see also Eq. (10) below].

[2)] When Coulomb scattering is neglected (which is not justified for energies near 50 MeV) the cross sections at $\varepsilon = 0$ have extremely deep minima, and at $\varepsilon = -0.25$ the calculated $\bar{p}^{12}C$ cross section accidentally coincides with the experimental data (see Ref. 4). When Coulomb scattering is neglected, the cross sections for scattering on ^{40}Ca and ^{208}Pb (Ref. 1) cannot be described at any value of ε.

[3)] According to the preliminary LEAR data,[59] $\Delta E_{3,2}(^{16}O) = (120 \pm 20)$ eV.

[1] D. Garreta, P. Birien, G. Bruge *et al.*, Phys. Lett. **B135**, 266 (1984); **B139**, 464 (1984); **B149**, 64 (1984).
[2] R. J. Glauber, in: *Lectures in Theoretical Physics*, Vol. 1, edited by W. E. Brittin and L. G. Dunham (Interscience, New York, 1959), p. 315.
[3] A. G. Sitenko, Ukr. Fiz. Zh. **4**, 152 (1959); *Theory of Nuclear Reactions* [in Russian] (Énergoatomizdat, Moscow, 1983).
[4] O. D. Dal'karov and V. A. Karmanov, Pis'ma Zh. Eksp. Teor. Fiz. **39**, 288 (1984) [JETP Lett. **39**, 345 (1984)]; Zh. Eksp. Teor. Fiz. **89**, 1122 (1985) [Sov. Phys. JETP **62**, 645 (1985)]; Phys. Lett. **B147**, 1 (1984); Nucl. Phys. **A445**, 579 (1985); Preprints No. 77 (1984), No. 55 (1985), No. 75 (1985), Lebedev Physical Institute, Moscow.
[5] "$\bar{N}N$ and $\bar{N}D$ interactions—a compilation," **LBI-58**, Berkeley (1972).
[6] A. K. Kerman, M. McManus, and R. M. Thaler, Ann. Phys. (N.Y.) **8**, 551 (1959).
[7] L. D. Dakhno and N. N. Nikolaev, Nucl. Phys. **A436**, 653 (1985).
[8] O. D. Dalkarov, V. M. Kolybasov, and V. G. Ksenzov, Nucl. Phys. **A397**, 498 (1983).
[9] T. A. Osborn, Ann. Phys. (N.Y.) **58**, 417 (1970).
[10] K. Gottfried, Ann. Phys. (N.Y.) **66**, 868 (1971).
[11] G. Fäldt, Nucl. Phys. **B46**, 460 (1972).
[12] M. S. Marinov, *The Coherent Interaction of High Energy Particles with Nuclei* [in Russian] (Moscow Engineering Physics Institute Press, Moscow, 1972).
[13] V. M. Kolybasov and L. A. Kondratyuk, Yad. Fiz. **18**, 316 (1973) [Sov. J. Nucl. Phys. **18**, 162 (1974)]; Phys. Lett. **B39**, 439 (1972).
[14] L. A. Kondratyuk, in: *Interaction of High Energy Particles with Nuclei and New Nucleus-Like Systems* [in Russian] (Atomizdat, Moscow, 1972), p. 5.
[15] S. Y. Wallace, Ann. Phys. (N.Y.) **78**, 190 (1973).
[16] S. P. Manaenkov, Yad. Fiz. **27**, 352 (1978) [Sov. J. Nucl. Phys. **27**, 190 (1978)].
[17] G. D. Alkhazov, S. L. Belostotsky, and A. A. Vorobyov, Phys. Rep. **42C**, 89 (1978).
[18] O. D. Dalkarov and F. Myhrer, Nuovo Cimento **A40**, 152 (1977).
[19] I. S. Shapiro, Phys. Rep. **35C**, 129 (1978).
[20] W. Brückner, H. Döbbeling, F. Güttner *et al.*, Phys. Lett. **B166**, 113 (1986).
[21] Y. Pumplin, Phys. Rev. **173**, 1651 (1968).
[22] L. A. Kondratyuk, M. Zh. Shmatikov, and R. Bidzarri, Yad. Fiz. **33**, 795 (1981) [Sov. J. Nucl. Phys. **33**, 413 (1981)].
[23] L. A. Kondratyuk and M. G. Sapozhnikov, in: *Proceedings of the 20th Winter School of the Leningrad Institute of Nuclear Physics* [in Russian] (1985), p. 298.
[24] D. Brückner, H. Döbbeling, F. Güttner *et al.*, Phys. Lett. **B158**, 180 (1985).
[25] R. D. Tripp, in: *Proceedings of the Fifth European Symposium on Nucleon–Antinucleon Interactions* (Bressanone, Italy, June 23–28, 1980), p. 519.
[26] R. H. Bassel and C. Wilkin, Phys. Rev. **174**, 1179 (1968).
[27] R. Hofstadter, Ann. Rev. Nucl. Sci. **7**, 231 (1957).
[28] O. D. Dal'karov, V. A. Karmanov, and A. V. Trukhov, Yad. Fiz. **45**, 688 (1987) [Sov. J. Nucl. Phys. **45**, 430 (1987)].
[29] M. Cresti, L. Peruzzo, and G. Sartori, Phys. Lett. **B132**, 209 (1983).
[30] V. Ashford, M. E. Sainio, M. Sakitt *et al.*, Phys. Rev. Lett. **54**, 518 (1985).
[31] N. Nakamura, Y. Chiba, T. Fujii *et al.*, Phys. Rev. Lett. **52**, 731 (1984).
[32] V. Ashford, M. E. Sainio, M. Sakitt *et al.*, Phys. Rev. C **30**, 1080 (1984).
[33] G. Alberi, R. Birsa, F. Bradamante *et al.*, in: *Proceedings of the Fifth European Symposium on Nucleon–Antinucleon Interactions* (Bressanone, Italy, June 23–28, 1980), p. 51.
[34] M. Kaseno, R. Haigatsu, K. Kawano *et al.*, Phys. Lett. **B61**, 203 (1976).
[35] G. Bruge, A. Chaumeaux, P. Biren *et al.*, Phys. Lett. **B169**, 14 (1986).
[36] J. A. Niskanen and A. M. Green, Nucl. Phys. **A404**, 495 (1983).
[37] T. Suzuki, Nucl. Phys. **A444**, 659 (1985).
[38] H. V. Von Geramb and L. Rikus, in: *Proceedings of the Tenth International Conference on Particles and Nuclei*, Part G9 (Heidelberg, July 30–August 3, 1984), p. 10.
[39] C. J. Batty, E. Friedman, and J. Lichtenstadt, Phys. Lett. **B142**, 241 (1984).

[40]K. I. Kubo, H. Toki, and M. Igarashi, Nucl. Phys. **A435**, 708 (1985).
[41]C. J. Batty, E. Friedman, and J. Lichtenstadt, Nucl. Phys. **A436**, 621 (1985).
[42]J. Lichtenstadt, A. I. Yavin, S. Janoulin *et al.*, Phys. Rev. C **32**, 1096 (1985).
[43]F. Balestra, S. Bossolasco, M. P. Bussa *et al.*, Nucl. Phys. **A452**, 573 (1986).
[44]V. V. Balashov, in: *Proceedings of the Eighth Winter School of the Leningrad Institute of Nuclear Physics*, Part 2 (Leningrad, 1973), p. 255; V. N. Mileev and T. V. Mischenko, Phys. Lett. **B47**, 197 (1973).
[45]L. A. Kondratyuk and Yu. A. Simonov, Pis'ma Zh. Eksp. Teor. Fiz. **17**, 619 (1973) [JETP Lett. **17**, 435 (1973)]; in: *Elementary Particles: Proceedings of the Second IHEP Physics School*, No. 1 [in Russian] (Atomizdat, Moscow, 1975), p. 72.
[46]M. Bouten and P. van Leuven, Ann. Phys. (N.Y.) **43**, 421 (1967).
[47]A. N. Antonov and E. V. Inopin, Yad. Fiz. **16**, 74 (1972) [Sov. J. Nucl. Phys. **16**, 38 (1973)].
[48]I. V. Kirpichnikov, V. A. Kuznetsov, I. I. Levintov, and A. S. Starostin, Yad. Fiz. **41**, 21 (1985) [Sov. J. Nucl. Phys. **41**, 13 (1985)]; Preprints ITEP-96 (1979), ITEP-96 (1984) [in Russian], Moscow; I. V. Kirpichnikov, V. A. Kuznetsov, and A. S. Starostin, Yad. Fiz. **40**, 1377 (1984); **41**, 18 (1985) [Sov. J. Nucl. Phys. **40**, 875 (1984); **41**, 11 (1985)]; Preprints ITEP-119 (1981), ITEP-94 (1984), ITEP-95 (1984) [in Russian], Moscow.
[49]V. A. Karmanov, Yad. Fiz. **35**, 848 (1982) [Sov. J. Nucl. Phys. **35**, 492 (1982)].
[50]O. D. Dal'karov and V. G. Ksenzov, Yad. Fiz. **32**, 1439 (1980) [Sov. J. Nucl. Phys. **32**, 744 (1980)].
[51]O. D. Dal'karov, Pis'ma Zh. Eksp. Teor. Fiz. **28**, 183 (1978) [JETP Lett. **28**, 170 (1978)].
[52]F. Balestra, Yu. A. Batusov, G. Bendiscioli *et al.*, in: *Proceedings of the Seventh European Symposium on Antiproton Interactions* (Durham, 1984), p. 251; Nucl. Phys. **A452**, 573 (1986); Phys. Lett. **B165**, 265 (1985).
[53]Yu. A. Batusov *et al.*, Kratk. Soobshch. OIYaI, No. 6-85, 11 (1985).
[54]M. Yu. Khlopov, Priroda **5**, 20 (1985).
[55]M. G. Sapozhnikov, Priroda **6**, 70 (1985).
[56]E. Lambert, Helv. Phys. Acta **42**, 667 (1969).
[57]P. Robertson, T. King, R. Kunselman *et al.*, Phys. Rev. C **16**, 1945 (1977).
[58]H. Poth, G. Backenstoss, T. Bergström *et al.*, Nucl. Phys. **A294**, 435 (1978).
[59]H. Poth, P. Blüm, G. Büche *et al.*, Preprint CERN-EP/85-75, CERN, Geneva (1985).
[60]B. O. Kerbikov, V. G. Ksenzov, and A. C. Kudryavtsev *et al.*, Preprint ITEP-61, Moscow (1978).
[61]H. Iwasaki, H. Aihara, J. Chiba *et al.*, Phys. Lett. **B103**, 247 (1981); Nucl. Phys. **A433**, 580 (1985).
[62]H. Kaseno, R. Hamatsu, K. Kowano *et al.*, Phys. Lett. **B61**, 203 (1976); **B68**, 487 (1977).
[63]A. M. Green and J. A. Niskanen, Preprint No. HU-TFT-85-60, University of Helsinki (1985).
[64]C. Dover and J. M. Richard, Phys. Rev. C **21**, 1466 (1980).
[65]A. M. Green and J. A. Niskanen, Nucl. Phys. **A430**, 605 (1984).
[66]M. Maruyama and T. Ueda, Prog. Theor. Phys. **74**, 526 (1985).
[67]J. M. Eisenberg, Ann. Phys. (N.Y.) **71**, 542 (1972).
[68]V. M. Chechetkin, M. Yu. Khlopov, and M. G. Sapozhnikov, Riv. Nuovo Cimento **5**, No. 5 (1982); I. V. Falomkin, G. B. Pontecorvo, M. G. Sapozhnikov *et al.*, Nuovo Cimento **A79**, 193 (1984); Y. A. Batusov, I. V. Falomkin, G. B. Pontecorvo *et al.*, Lett. Nuovo Cimento **41**, 223 (1984); Y. Ellis, D. V. Nanopoulos, S. Sarkar *et al.*, Nucl. Phys. **B259**, 175 (1985).
[69]K. Miyano, Y. Noguchi, M. Fukawa *et al.*, Phys. Rev. Lett. **53**, 1725 (1984).
[70]G. Piragino, Preprint CERN-EP/86-75, CERN, Geneva (1986).
[71]V. P. Zavarzina and V. A. Sergeev, Preprint P-0505 [in Russian], Institute for Nuclear Research, USSR Academy of Sciences, Moscow (1986).

Translated by Patricia Millard